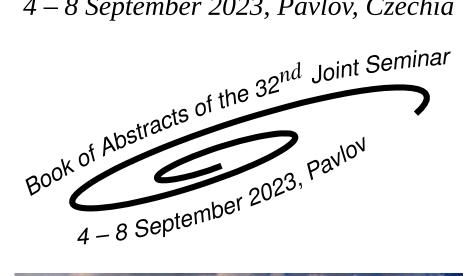
### **DMSRE 2023**

### **Development of Materials Science** in Research and Education

4 – 8 September 2023, Pavlov, Czechia





### **Organized** by

Czechoslovak Association for Crystal Growth Slovak Expert Group of Solid State Chemistry and Physics

### Under the auspicies of

*Institute of Physics of the Czech Academy of Sciences Slovak Society for Industrial Chemistry* Faculty of Chemical and Food Technology STU in Bratislava Faculty of Materials Science and Technology STU in Trnava

# Development of Materials Science in Research and Education

4 – 8 September 2023, Pavlov, Czechia

### Book of Abstracts of the 32<sup>nd</sup> Joint Seminar

### **Topics**

- Trends in development of materials research
- Information about the research programs of individual institutions
- · Results of materials research
- Education of materials science at the universities
- Information about equipment for preparation and characterisation of materials





#### Scientific Committee

Jaromír Drápala, Technical University of Ostrava, Ostrava
Jan Grym, Institute of Photonics and Electronics, Prague
Marian Koman, Slovak University of Technology in Bratislava, Bratislava (co-chair)
Zdeněk Kožíšek, Institute of Physics of the Czech Academy of Sciences, Prague (chair)
Vladimír Kuchtanin, Slovak University of Technology in Bratislava, Bratislava
Maroš Martinkovič, Faculty of Material Science and Technology SUT, Trnava

Mária Behúlová, Faculty of Material Science and Technology SUT, Trnava

Petr Mošner, University of Pardubice, Pardubice

Jan Polák, Crytur Turnov, Turnov

Zdeněk Potůček, Faculty of Nuclear Sciences and Physical Engineering CTU, Prague Kateřina Rubešová, University of Chemistry and Technology, Prague

### **Organizing Committee**

Zdeněk Kožíšek, Institute of Physics of the Czech Academy of Sciences, Prague (chairman)
Mária Behúlová, Faculty of Material Science and Technology SUT, Trnava
Aleš Bystřický, Institute of Physics of the Czech Academy of Sciences, Prague
Robert Král, Institute of Physics of the Czech Academy of Sciences, Prague
Zdeňka Poláčková, Institute of Physics of the Czech Academy of Sciences, Prague
Vojtěch Vaněček, Institute of Physics of the Czech Academy of Sciences, Prague
Petra Zemenová, Institute of Physics of the Czech Academy of Sciences, Prague

Supported by the Czechoslovak Association for Crystal Growth (CSACG) CZ-162 00 Prague 6, Cukrovarnická 10, Czech Republic

Published by the Institute of Physics of the Czech Academy of Sciences, v. v. i. CZ-182 21 Prague 8, Na Slovance 1999/2, Czech Republic

Editors: Zdeněk Kožíšek, Robert Král, and Petra Zemenová

ISBN 978-80-907237-4-0

#### **PREFACE**

The 32<sup>nd</sup> Joint Seminar "Development of Materials Science in Research and Education" (DMSRE32) will be held on 4 – 8 September 2023, in hotel IRIS Pavlov. The first Joint Seminar in these series was held at Gabčíkovo in Czechoslovakia in 1991. Seminar is organized by the Czechoslovak Association for Crystal Growth and the Slovak Expert Group of Solid State Chemistry and Physics under the auspicies of the Institute of Physics of the Czech Academy of Sciences, Faculty of Chemical and Food Technology SUT Bratislava, and Slovak Society for Industrial Chemistry every year with one break in 2021 (COVID-19 pandemic).

The Seminar brings together a unique combination of scientists across a multidisciplinary spectrum and provides an ideal forum for the presentations and discussions of recent developments and achievements in all theoretical and experimental aspects of preparation processes, characterization and applications of materials in bulk, thin film, nano-crystalline and glassy states.

The program will include 4 keynote lectures (35 minutes): Maksym Buryi (Institute of Physics of the Czech Academy of Sciences, Prague, Czechia) *Point defects creation and their influence on luminescent properties of 0D, 1D, 2D and 3D materials*, Kei Kamada (Tohoku University, Sendai, Japan) *Development and material design of structured scintillators for high resolution radiation imaging and thermal neutron detection*, Milos Nesladek (Hasselt University, Belgium) *NV spin qubit systems: a platform from sensing to quantum computation*, and Michal Piasecki (Jan Dlugosz University in Czestochowa, Czestochowa, Poland) *Metal Chalcogenides for Thermoelectricity, Solar Cells and Optoelectronic Devices*.

All other contributions will be presented as short lecture talks (20 minutes including discussion). The official languages of the seminar are English, Czech, and Slovak.

This booklet contains the abstracts of all contributions, which reached us before 16 August 2023. The authors are responsible for the technical and language quality of the contributions. The conference will run from Monday afternoon, 4 September 2023, untill Friday noon, 8 September 2023 in the hotel IRIS Pavlov, Czech Republic.

Dear colleagues, we welcome you to the  $32^{nd}$  DMSRE Joint Seminar and we hope you will enjoy your stay in Pavlov.

Zdeněk Kožíšek, Robert Král, and Petra Zemenová (Editors)

### **CONTENT**

| Program   |
|---|
| Abstracts13   |
| Crystal growth of Eu-doped (Y, Lu)ScO <sub>3</sub> by micro-pulling-down method using W crucible15 <u>Yuka Abe</u> , Takahiko Horiai, Yuui Yokota, Masao Yoshino, Rikito Murakami, Takashi Hanada, Akihiro Yamaji, Hiroki Sato, Yuji Ohashi, Shunsuke Kurosawa, Kei Kamada, and Akira Yoshikawa |
| Assessment of the impact of process parameters on temperature fields during laser cutting of AISI 304 steel sheets  |
| Characterization of different types of silica-based materials   |
| Preparation and characterization of gold nanoparticles in silicate glass matrices using aerodynamic levitation coupled to laser heating   |
| Highly nonstoichiometric $Tb_2Y_{0.1-1}Al_5O_{12}$ :Ce single crystals with modified microstructure, defect concentration, luminescence, and scintillation properties   |
| Heat source models for numerical simulation of laser welding processes20 <u>Mária Behúlová</u> and Eva Babalová   |
| Point defects creation and their influence on luminescent properties of 0D, 1D, 2D and 3D materials 21 <u>Maksym Buryi</u> , Vladimir Babin, František Hájek, Tomáš Hubáček, Anna Artemenko, Zdeněk Remeš and Júlia Mičová  |
| Extreme Large 2D and 3D Nanoscale Application   |
| Study of phase equilibria in Al-Co and Pd-Co systems23 <u>Ivona Černičková</u> , Libor Ďuriška, Peter Švec sr., and Jozef Janovec   |
| Analysis of phase transformations in Fe - 1.1C - 0.9Si – 0.4Mn – 8.3Cr – 2.1 Mo – 0.5V steel using dilatometry and computational thermodynamics   |
| Ion Beam Analysis including ToF ERDA of complex composition layers  |
| A measuring of the sound absorption coefficient of structured materials produced by 3D printing26 <u>Rastislav Ďuriš</u> and Eva Labašová   |
| Structural, thermal and mechanical properties of gallium-enriched SAC lead-free solders27 <u>Libor Ďuriška</u> , Ivona Černičková, Marián Drienovský, Roman Moravčík, Ladislav Dobrovodský, and Roman Čička   |

| Analysis of Biocompatible Metallic Materials used in Medicine  |
|--|
| Basic study of lithium strontium borates as thermal neutron scintillators  |
| Crystal growth and optical characterization of Ce-doped mixed rare-earth sesquioxide single crystals for scintillator applications   |
| Structure and properties of $Ag_2O$ - $GeO_2$ - $P_2O_5$ glasses   |
| The influence of structure, sensitization and corrosion on the fatigue properties of AISI 304 austenitic steel   |
| Y-stabilized hafnia as a potential scintillating material for ionizing radiation detection33 <u>Vít Jakeš</u> , Kateřina Rubešová, Tomáš Thoř, Jiří Prikner, Christo Guguschev, Romana Kučerková, Jan Pejchal, and Martin Nikl |
| Advances in hydroxyapatite dosimetry: New trends   |
| Influence the effect of balancing the grinding set on the accuracy and roughness of the machined surface   |
| Development and material design of structured scintillators for high resolution radiation imaging and thermal neutron detection  |
| The Effect of the Laser Beam on the width of the Cut   |
| The role of X-ray radiation in materials research  |
| Experience with modeling values of the virtual catapult range  |
| Silver phosphate glasses modified by transition metal oxides   |
| Energy of nuclei formation on curved active centers  |
| Simultaneous DSC-TGA-MS analyses of $RE_2O_3$ compounds for growth multicomponent oxides42 <u>Robert Král</u> , Petra Zemenová, Alexandra Falvey, Vojtěch Vaněček, Aleš Bystřický, Jan Pejchal, and Martin Nikl                |
| Statistical evaluation of hard-to-measure surfaces   |

| New Ni(II) complexes with 2-aminomethylbenzimidazole, preparation and characterization 44<br><u>Vladimír Kuchtanin,</u> Rudolf Varga, Ján Pavlik, and Ján Moncol'  |
|--|
| Development of a high-frequency rapid scan electron spin resonance spectrometer45<br>Oleksii Laguta, Matuš Šedivý, Vinicius Santana, Andriy Marko , and Petr Neugebauer  |
| Activation function as an inspiration for metamaterial design and gyroid as inspiration for activation function design. Part 2: next contexts  |
| Degradation of rubber compounds under natural conditions   |
| Possible methods of removing PCBs from environment48  Jaroslava Maroszová  |
| Possibilities of analyzing the mechanical properties of welded and soldered joints   |
| Single crystal gowth of Ru-Mo-W-Re alloy wire by the dewetting micro-pulling-down method 50 <u>Rikito Murakami</u> , Shiika Itoi, Kotaro Yonemura, Kei Kamada, and Akira Yoshikawa                             |
| Effect of structural modification of rotor with a flexible shaft on its modal properties51<br>Milan Nad', Peter Bucha, and Ladislav Rolník   |
| Assessment of cutting tool wear using a numerical FEM simulation model   |
| NV spin qubit systems: a platform from sensing to quantum computation53  Milos Nesladek  |
| Crystal Growth and Optical Properties of Ce-doped (Y, Tb) <sub>3</sub> Al <sub>2</sub> Ga <sub>3</sub> O <sub>12</sub> and (Gd, Tb) <sub>3</sub> Al <sub>2</sub> Ga <sub>3</sub> O <sub>12</sub> Scintillators |
| Influence of selected parameters of drag finishing on tool microgeometry55<br>Boris Pätoprstý, Marek Vozár, Tomáš Vopát, Ivan Buranský, and František Jurina   |
| Morphology of selected multicomponent garnet laser crystals grown by micro-pulling-down method 56<br>Jan Pejchal, Jan Havlíček, Jan Šulc, Karel Nejezchleb, Helena Jelínková, and Martin Nikl                  |
| Metal Chalcogenides for Thermoelectricity, Solar Cells and Optoelectronic Devices  |
| Bioactivity of carboxylatocopper(II) complexes58<br><u>Miroslava Puchoňová</u> and Flóra Jozefíková  |
| The comparison of photoluminescence decay in YAG:Er, ZnO and SiO <sub>2</sub> crystals59<br><u>Zdeněk Remeš,</u> Maksym Buryi, Štěpán Remeš, Radim Novák, Jan Pejchal, Oleg Babčenko, and Júlic<br>Mičová      |
| How many electronic study resources is too much?60<br>Kateřina Rubešová and Vít Jakeš  |

| parts   |
|---|
| <u>Martin Sahul</u> , Miroslav Sahul, Ladislav Kolařík, Tomáš Němec, Marie Kolaříková, and Barbora Bočáková   |
| Influence of generator parameters on cutting width during WEDM process  |
| Tribological performance of nanolaminate coatings based on tungsten and niobium nitrides63 <u>Kateryna Smyrnova</u> , Martin Sahul, Marián Haršáni, Alexander Pogrebnjak, Lubomír Čaplovič, Vyacheslav Beresnev, Mária Čaplovičová, and Martin Kusy |
| Transparent ceramics of $LiAl_5O_8$ prepared by spark plasma sintering  |
| The influence of heat treatment on the nitriding layear on AISI 304 austenitic steel  |
| Development of novel cross-luminescence scintillators   |
| Er-doped zinc-silicate glass-ceramics with enhanced emission in the near-infrared region67 <u>Petr Vařák</u> , Jan Baborák, Emmanuel Véron, Alena Michalcová, Jan Mrázek, Jakub Volf, Mathieu Allix, and Pavla Nekvindová                           |
| The effect of composition on luminescence properties of Ce and Mn ions in borate-silicate glasses 68 <u>Jakub Volf, Petr Vařák, Martin Kormunda, Maksym Buryi, and Pavla Nekvindová</u>   |
| Development of cutting forces in high-speed machining on turning centre   |
| Influence of cutting edge microgeometry on the selected aspects of machining difficult-to-cut materials   |
| Composition Dependence of Resistivity of Ru-Mo-W ternary system and single crystal wire growth by the dewetting micro-pulling-down method   |
| Corrosion resistance of austenitic stainless steels in mixed sulfuric acid and copper sulfate solution 72 <u>Viera Zatkalíková</u> , <i>Lenka Markovičová</i> , <i>Milan Uhríčik</i> , <i>and Silvia Hudecová</i>                                   |
| Author index  |
| List of Participants  |

### **PROGRAM**

### Monday, 4 September 2023

| 12:30                   | _ | 14:45                   | Registration  |
|-------------------------|---|-------------------------|---|
| 15:00                   | - | 15:05                   | Location: Hotel Lounge (near reception)  Opening  Location: Lecture Hall  |
| 15:05                   | _ | 16:00                   | Monday Session 1  Location: Lecture Hall  (chairperson: Zdeněk Kožíšek)   |
| 15:05                   | - | 15:40                   | Kei Kamada<br>Development and material design of structured scintillators for high resolution<br>radiation imaging and thermal neutron detection  |
| 15:40                   | _ | 16:00                   | Vojtěch Vaněček<br>Development of novel cross-luminescence scintillators  |
| 16:00                   | _ | 16:30                   | Coffee break  |
|                         |   |                         |   |
| 16:30                   | - | 18:10                   | Monday Session 2  Location: Lecture Hall  (chairperson: Mária Behúlová)   |
| 4.0.00                  | _ |                         | Location: Lecture Hall<br>(chairperson: Mária Behúlová)<br>Marian Koman   |
| 16:30                   | _ |                         | Location: Lecture Hall<br>(chairperson: Mária Behúlová)   |
| 16:30<br>16:50          | _ | 16:50                   | Location: Lecture Hall (chairperson: Mária Behúlová)  Marian Koman The role of X-ray radiation in materials research  Vladimír Kuchtanin New Ni(II) complexes with 2-aminomethylbenzimidazole, preparation and  |
| 16:30<br>16:50          | _ | 16:50<br>17:10          | Location: Lecture Hall (chairperson: Mária Behúlová)  Marian Koman The role of X-ray radiation in materials research  Vladimír Kuchtanin New Ni(II) complexes with 2-aminomethylbenzimidazole, preparation and characterization  Rastislav Ďuriš A measuring of the sound absorption coefficient of structured materials pro-   |
| 16:30<br>16:50<br>17:10 | - | 16:50<br>17:10<br>17:30 | Location: Lecture Hall (chairperson: Mária Behúlová)  Marian Koman The role of X-ray radiation in materials research  Vladimír Kuchtanin New Ni(II) complexes with 2-aminomethylbenzimidazole, preparation and characterization  Rastislav Ďuriš A measuring of the sound absorption coefficient of structured materials produced by 3D printing  Miroslava Puchoňová |

## Tuesday, 5 September 2023

| 00.45 |   | 10.00 | The adam Constant   |
|-------|---|-------|---|
| 08:45 | _ | 10:00 | Tuesday Session 1   |
|       |   |       | Location: Lecture Hall  |
|       |   |       | (chairperson: Maksym Buryi)   |
| 08:45 | - | 09:20 | Milos Nesladek NV spin qubit systems: a platform from sensing to quantum computation  |
| 09:20 | - | 09:40 | Zdeněk Remeš The comparison of photoluminescence decay in YAG:Er, ZnO and SiO $_2$ crystals   |
| 09:40 | - | 10:00 | Jakub Volf<br>The effect of composition on luminescence properties of Ce and Mn ions in<br>borate-silicate glasses  |
| 10:00 | - | 10:30 | Coffee break  |
| 10:30 | _ | 12:10 | Tuesday Session 2   |
|       |   |       | Location: Lecture Hall  |
|       |   |       | (chairperson: Kei Kamada)   |
| 10:30 | - | 10:50 | Takahiko Horiai<br>Crystal growth and optical characterization of Ce-doped mixed rare-earth<br>sesquioxide single crystals for scintillator applications        |
| 10:50 | - | 11:10 | Rikito Murakami<br>Single crystal gowth of Ru-Mo-W-Re alloy wire by the dewetting micro-pulling-<br>down method   |
| 11:10 | - | 11:30 | Kotaro Yonemura<br>Composition Dependence of Resistivity of Ru-Mo-W ternary system and single<br>crystal wire growth by the dewetting micro-pulling-down method |
| 11:30 | - | 11:50 | Kazuya Omuro Crystal Growth and Optical Properties of Ce-doped (Y, $Tb$ ) <sub>3</sub> $Al_2Ga_3O_{12}$ and $(Gd, Tb)_3Al_2Ga_3O_{12}$ Scintillators            |
| 11:50 | - | 12:10 | Yuka Abe Crystal growth of Eu-doped (Y, Lu)ScO $_3$ by micro-pulling-down method using W crucible   |
| 12:15 | _ | 13:15 | Lunch   |
| 14:00 | - | 15:40 | Tuesday Session 3  Location: Lecture Hall  (chairperson: Takahiko Horiai)   |
| 14:00 | - | 14:20 | Jan Pejchal Morphology of selected multicomponent garnet laser crystals grown by micropulling-down method   |

| 14:20 | - | 14:40 | Karol Bartosiewicz Highly nonstoichiometric $Tb_2Y_{0.1-1}Al_5O_{12}$ :Ce single crystals with modified microstructure, defect concentration, luminescence, and scintillation properties |
|-------|---|-------|--|
| 14:40 | - | 15:00 | Jan Havlíček<br>Basic study of lithium strontium borates as thermal neutron scintillators  |
| 15:00 | - | 15:20 | Vít Jakeš<br>Y-stabilized hafnia as a potential scintillating material for ionizing radiation<br>detection   |
| 15:20 | - | 15:40 | Robert Král Simultaneous DSC-TGA-MS analyses of $RE_2O_3$ compounds for growth multicomponent oxides   |
| 15:40 | _ | 16:10 | Coffee break   |
| 16:10 | _ | 18:10 | Tuesday Session 4  Location: Lecture Hall  (chairperson: Maroš Martinkovič)  |
| 16:10 | _ | 16:30 | Antonio Casares Extreme Large 2D and 3D Nanoscale Application  |
| 16:30 | - | 16:50 | Milan Nad'<br>Effect of structural modification of rotor with a flexible shaft on its modal prop-<br>erties  |
| 16:50 | - | 17:10 | František Jurina<br>Influence the effect of balancing the grinding set on the accuracy and roughness<br>of the machined surface  |
| 17:10 | _ | 17:30 | Tomáš Vopát<br>Development of cutting forces in high-speed machining on turning centre   |
| 17:30 | - | 17:50 | Marek Vozár<br>Influence of cutting edge microgeometry on the selected aspects of machining<br>difficult-to-cut materials  |
| 17:50 | _ | 18:10 | Tomáš Thoř Transparent ceramics of $LiAl_5O_8$ prepared by spark plasma sintering  |
| 18:15 | _ | 19:15 | Dinner   |

## Wednesday, 6 September 2023

| 08:45 | _ | 10:00 | Wednesday Session 1  |
|-------|---|-------|--|
|       |   |       | Location: Lecture Hall   |
|       |   |       | (chairperson: Jan Pejchal)   |
| 08:45 | _ | 09:20 | Maksym Buryi<br>Point defects creation and their influence on luminescent properties of 0D, 1D,<br>2D and 3D materials   |
| 09:20 | - | 09:40 | Oleksii Laguta<br>Development of a high-frequency rapid scan electron spin resonance spectrom-<br>eter                   |
| 09:40 | - | 10:00 | David John Advances in hydroxyapatite dosimetry: New trends  |
| 10:00 | _ | 10:30 | Coffee break   |
| 10:30 | _ | 12:10 | Wednesday Session 2  |
|       |   |       | Location: Lecture Hall   |
|       |   |       | (chairperson: Vladimír Kuchtanin)  |
| 10:30 | - | 10:50 | Maroš Martinkovič<br>Possibilities of analyzing the mechanical properties of welded and soldered<br>joints               |
| 10:50 | - | 11:10 | Martin Necpal<br>Assessment of cutting tool wear using a numerical FEM simulation model                                  |
| 11:10 | - | 11:30 | Martin Sahul<br>Effect of welding mode on selected properties of additively manufactured<br>AA5087 aluminium alloy parts |
| 11:30 | - | 11:50 | Vladimír Šimna<br>Influence of generator parameters on cutting width during WEDM process                                 |
| 11:50 | _ | 12:10 | Kateřina Rubešová<br>How many electronic study resources is too much?  |
| 12:15 | _ | 13:15 | Lunch  |
| 14:00 | _ | 17:00 | Joint meeting - panel discussion   |
|       |   |       | •  |
| 18:00 | _ | 19:00 | Dinner  Conference has seet  |
| 19:30 | _ | 23:30 | Conference banquet   |
|       |   |       | Location: Wine Vault   |

# Thursday, 7 September 2023

| 08:45 | _ | 10:00 | Thursday Session 1  |
|-------|---|-------|---|
| 00.45 |   | 10.00 | Location: Lecture Hall  |
|       |   |       | (chairperson: Zdeněk Remeš)   |
| 08:45 | - | 09:20 | Michal Piasecki<br>Metal Chalcogenides for Thermoelectricity, Solar Cells and Optoelectronic<br>Devices   |
| 09:20 | _ | 09:40 | Oleg Babčenko<br>Characterization of different types of silica-based materials  |
| 09:40 | _ | 10:00 | Libor Ďuriška<br>Structural, thermal and mechanical properties of gallium-enriched SAC lead-<br>free solders  |
| 10:00 | - | 10:30 | Coffee break  |
| 10:30 | _ | 12:10 | Thursday Session 2  |
|       |   |       | Location: Lecture Hall  |
|       |   |       | (chairperson: Vojtěch Vaněček)  |
| 10:30 | - | 10:50 | Ladislav Koudelka<br>Silver phosphate glasses modified by transition metal oxides   |
| 10:50 | - | 11:10 | Tomáš Hostinský Structure and properties of $Ag_2O$ - $GeO_2$ - $P_2O_5$ glasses  |
| 11:10 | - | 11:30 | Jan Baborák<br>Preparation and characterization of gold nanoparticles in silicate glass matri-<br>ces using aerodynamic levitation coupled to laser heating |
| 11:30 | - | 11:50 | Petr Vařák<br>Er-doped zinc-silicate glass-ceramics with enhanced emission in the near-<br>infrared region  |
| 11:50 | _ | 12:10 | Jozef Dobrovodský<br>Ion Beam Analysis including ToF ERDA of complex composition layers   |
| 12:15 | _ | 13:15 | Lunch   |
| 14:00 | _ | 16:00 | Thursday Session 3  |
|       |   |       | Location: Lecture Hall  |
|       |   |       | (chairperson: Miroslava Puchoňová)  |
| 14:00 | - | 14:20 | Lenka Markovičová  Degradation of rubber compounds under natural conditions   |
| 14:20 | - | 14:40 | Viera Zatkalíková<br>Corrosion resistance of austenitic stainless steels in mixed sulfuric acid and<br>copper sulfate solution                              |

| 14:40          | _ | 15:00          | Milan Uhríčik<br>The influence of structure, sensitization and corrosion on the fatigue properties<br>of AISI 304 austenitic steel   |
|----------------|---|----------------|--|
| 15:00          | - | 15:20          | Milan Uhríčik<br>The influence of heat treatment on the nitriding layear on AISI 304 austenitic<br>steel   |
| 15:20          | - | 15:40          | Jaroslava Maroszová<br>Possible methods of removing PCBs from environment  |
| 15:40          | _ | 16:00          | Boris Pätoprstý<br>Influence of selected parameters of drag finishing on tool microgeometry  |
| 16:00          | _ | 16:30          | Coffee break   |
| 16:30          | - | 17:50          | Thursday Session 4 (video session)  Location: Lecture Hall   |
|                |   |                | (chairperson: Zdeněk Kožíšek)  |
| 16:30          | _ | 16:50          | (chairperson: Zdeněk Kožíšek)  Iveta Markechová Activation function as an inspiration for metamaterial design and gyroid as inspiration for activation function design. Part 2: next contexts  |
| 16:30<br>16:50 |   | 16:50<br>17:10 | Iveta Markechová<br>Activation function as an inspiration for metamaterial design and gyroid as  |
|                |   |                | Iveta Markechová Activation function as an inspiration for metamaterial design and gyroid as inspiration for activation function design. Part 2: next contexts Janette Kotianová   |
| 16:50          | _ | 17:10<br>17:30 | Iveta Markechová Activation function as an inspiration for metamaterial design and gyroid as inspiration for activation function design. Part 2: next contexts  Janette Kotianová Experience with modeling values of the virtual catapult range Žaneta Gerhátová |

### Friday, 8 September 2023

| 09:00                  | _ | 10:00 | Friday Session 1  |
|------------------------|---|-------|---|
| 05.00                  |   | 10.00 | Location: Lecture Hall  |
|                        |   |       | (chairperson: Kateřina Rubešová)  |
| 09:00                  | _ | 09:20 | Zdeněk Kožíšek<br>Energy of nuclei formation on curved active centers   |
| 09:20                  | - | 09:40 | Ivona Černičková<br>Study of phase equilibria in Al-Co and Pd-Co systems  |
| 09:40                  | _ | 10:00 | Roman Čička Analysis of phase transformations in Fe - $1.1C$ - $0.9Si$ – $0.4Mn$ – $8.3Cr$ – $2.1$ $Mo$ – $0.5V$ steel using dilatometry and computational thermodynamics |
| 10:00                  | - | 10:30 | Coffee break  |
| 10:30                  | _ | 11:50 | Friday Session 2  |
| Location: Lecture Hall |   |       |   |
|                        |   |       | (chairperson: Vít Jakeš)  |
| 10:30                  | _ | 10:50 | Mária Behúlová<br>Heat source models for numerical simulation of laser welding processes  |
| 10:50                  | - | 11:10 | Eva Babalová<br>Assessment of the impact of process parameters on temperature fields during<br>laser cutting of AISI 304 steel sheets                                     |
| 11:10                  | - | 11:30 | Jana Knedlová<br>The Effect of the Laser Beam on the width of the Cut   |
| 11:30                  | - | 11:50 | Milena Kubišová<br>Statistical evaluation of hard-to-measure surfaces   |
| 11:50                  | _ | 12:00 | Closing   |
| 12:00                  | _ | 13:00 | Lunch   |

### **ABSTRACTS**

## Crystal growth of Eu-doped (Y, Lu)ScO<sub>3</sub> by micro-pulling-down method using W crucible

<u>Yuka Abe</u><sup>1,2</sup>, Takahiko Horiai<sup>2,3</sup>, Yuui Yokota<sup>2,3</sup>, Masao Yoshino<sup>2,3</sup>, Rikito Murakami<sup>2</sup>, Takashi Hanada<sup>2</sup>, Akihiro Yamaji<sup>2,3</sup>, Hiroki Sato<sup>2,3</sup>, Yuji Ohashi<sup>2,3</sup>, Shunsuke Kurosawa<sup>2,3</sup>, Kei Kamada<sup>2,3</sup>, and Akira Yoshikawa<sup>2,3</sup>

<sup>1</sup>Graduate School of Engineering, Tohoku University, Japan
<sup>2</sup>Institute for Materials Research, Tohoku University, Japan
<sup>3</sup>New Industry Creation Hatchery Center, Tohoku University, Japan

**Introduction** The luminescence thermometry has drown considerable attention because of its fast response and applicability in harsh environments and high electromagnetic fields [1]. In particular, rare-earth ion doped  $Y_3Al_5O_{12}$  (YAG) has been widely studied and is expected to be used in the luminescence thermometry. For example, the temperature dependence of the decay time of Eu-doped YAG has been investigated and it was shown that temperatures can be accurately measured in the temperature range from 1000 K to 1470 K [2]. To further improve the properties, we focused on the sesquioxide such as  $Sc_2O_3$ ,  $Y_2O_3$  and  $Lu_2O_3$ , which have been reported to have higher thermal conductivity than YAG. Thus, in this study, we grew Eu-doped (Y, Lu) $ScO_3$ , crystals with Lu substitution at the Y site of YScO $_3$  and evaluated the effect of Lu substitution on the crystal structure and optical properties.

**Materials and Methods** The crystal growth was performed using micro-pulling-down ( $\mu$ -PD) method [3]. Y<sub>2</sub>O<sub>3</sub>, Lu<sub>2</sub>O<sub>3</sub>, Sc<sub>2</sub>O<sub>3</sub> and Eu<sub>2</sub>O<sub>3</sub> powders were used as starting materials and sintered at 1700°C for 30 hours in air. The sintered compacts were filled into the W crucible, and the crystals were grown using metal W rod as seed crystal at a pulling down rate of 0.05 mm/min. The crystal structure of the grown crystals were estimated by the powder X-ray diffraction (XRD) analysis. In addition, the photoluminescence (PL) excitation and emission spectra were measured and the effect of Lu substitution on emission was evaluated.

**Results** Transparent Eu:(Y, Lu)ScO<sub>3</sub> crystals were succeeded in growing. From the results of the powder XRD patterns, the crystalline system and space group of the grown crystals were identified cubic and Ia-3, respectively. PL emission spectra were measured in the wavelength range of 275-750 nm with excitation at 253 nm. From the PL emission spectrum, the sharp emission peaks due to the Eu<sup>3+</sup> 4f-4f transitions from  ${}^5D_0$  to lower lying  ${}^7F_J$  levels were observed. Details of the crystal structure and optical properties of Eu-doped (Y, Lu)ScO<sub>3</sub> crystals will be presented.

- [1] X. Wang, et al., Luminescent probes and sensors for temperature, Chem. Soc. Rev., 42 (2013) 7834–7869.
- [2] T. Kissel, et al., Phosphor thermometry: On the synthesis and characterisation of  $Y_3Al_5O_{12}$ :Eu (YAG:Eu) and YAlO<sub>3</sub>:Eu (YAP:Eu). Mater. Chem. Phys., 140 (2013) 435–440.
- [3] A. Yoshikawa, et al., Challenge and study for developing of novel single crystalline optical materials using micro-pulling-down method. Opt. Mater., 30 (2007) 6–10.

# Assessment of the impact of process parameters on temperature fields during laser cutting of AISI 304 steel sheets

#### Eva Babalová and Mária Behúlová

Slovak University of Technology in Bratislava, Faculty of Materials Science and Technology in Trnava, ul. Jána Bottu Č. 2781/25, Trnava 91724, Slovakia

Laser cutting has experienced significant advancements in recent times. Consequently, this technique now boasts exceptional precision and high cutting speed [1]. In  $CO_2$  laser cutting, the quality of the final product is primarily determined by the input parameters, including laser power, cutting speed, and assist gas pressure. Within the laser cutting process, the size of the heat affected zone (HAZ) is significantly influenced by both laser power and assist gas pressure. These two parameters play a pivotal role in both material melting and the ejection of molten material from the cutting aperture [2].

The consumption of the cutting medium depends on the laser focus position and the relationship between the assist gas pressure and the output nozzle diameter. These parameters collectively define the overall quality of the cuts. To decrease assist gas consumption along with preserving the desired cut quality, it is recommended to decrease the nozzle diameter and simultaneously increase the gas pressure [3].

The article is focused on the investigation of the influence of nitrogen assist gas pressure on temperature fields developed during a cutting process using numerical simulation. A simulation model was developed for the laser cutting process of a test specimen made from AISI 304 steel, with dimensions of  $50 \times 35 \times 2$  mm. The material properties for AISI 304 steel were determined using the JMatPro software. The conical heat source model was employed to describe the power input from the moving laser beam source to the cutting material. The sample cooling by free convection and radiation to the surrounding air and the nitrogen jet impingement was taken into account. Various available correlations [4] were utilized to calculate the heat transfer coefficient during a nitrogen gas jet cooling and their results compared. Finally, a series of numerical experiments was conducted using ANSYS software to evaluate the impact of the assist nitrogen gas pressure on temperature fields during the cutting process.

- [1] Li, M, Infrared Phys Technol 118 (2021) 103896.
- [2] Oh S Y et al. Opt Laser Technol 119 (2019) 105607.
- [3] Musil V et al. MM Science Journal, June 2018 (2018) 2363-2366.
- [4] N. Zuckerman and N. Lior, Jet Impingement Heat Transfer: Physics, Correlations, and Numerical Modeling, edited by G A Greene, J P Hartnett, A Bar-Cohen, Y I Cho, Advances in Heat Transfer, Elsevier, Vol 39 (2006) 565-631, ISSN 0065-2717.

#### Characterization of different types of silica-based materials

Oleg Babčenko<sup>1</sup>, Zdeněk Remeš<sup>1</sup>, Klára Beranová<sup>1</sup>, Kateřina Kolářová<sup>1</sup>, Jan Čermák<sup>1</sup>, Alexander Kromka<sup>1</sup>, Zdeněk Prošek<sup>2</sup>, and Pavel Tesárek<sup>2</sup>

<sup>1</sup>FZU – Institute of Physics of the Czech Academy of Sciences, Cukrovarnická 10/112, 162 00 Prague 6, Czech Republic

<sup>2</sup>Faculty of Civil Engineering, Czech Technical University in Prague, Thákurova 7, 166 29 Prague 6, Czech Republic

Glasses based on the silicon dioxide (silica) are able to retain their properties even when recycled and therefore belong to the one of the most demanded secondary raw materials. Regardless of their type, these waste glasses are commonly referred to as Si-based secondary raw materials. However, depending on the source of original waste, the properties and composition of milled glass powders vary affecting further usage. Therefore, a comprehensive characterization is essential in some cases.

In this study we investigate several commercially available silica-based granular materials (powders). These materials were analyzed in terms of their surface and/or bulk modification by plasma treatment, annealing or chemical processing. In particular, powders were characterized using attenuated total reflectance Fourier transform infrared spectroscopy, infrared Raman spectroscopy, energy-dispersive X-ray spectroscopy, the X-ray photoelectron spectroscopy, etc. The differences found in the primary structure of SiO<sub>2</sub> particles (amorphous vs crystalline) and the impurities content were considered as determinative factors for particles' surface modification (e.g. by hydroxyl groups). These results provide a fundamental background that contributes to a better understanding and explanation of the interaction reactions of Si-based secondary raw materials used as fillers in alkali-activated cement-based composite materials.

# Preparation and characterization of gold nanoparticles in silicate glass matrices using aerodynamic levitation coupled to laser heating

<u>Jan Baborák</u><sup>1,2</sup>, Petr Vařák<sup>1</sup>, Alessio Zandona<sup>2</sup>, Michael Pitcher<sup>2</sup>, Mathieu Allix<sup>2</sup>, Emmanuel Veron<sup>2</sup>, and Pavla Nekvindová<sup>1</sup>

In our contribution, aerodynamic levitation coupled to laser heating (ADL) technique was applied to synthetise silicate glasses samples containing gold nanoparticles. ADL is a device developed for studying thermophysical properties, molten oxide structure, microgravity, and new chemical phases. ADL melting has many advantages compared to traditional melt-quenching. The most significant in our opinion is that it is containerless (i.e., it minimizes heterogeneous nucleation) and it can attain extreme melting temperatures up to 3000 °C, beyond the melting point of most oxide materials. However, these advantages are balanced with some disadvantages, such as the easy loss of volatile components during melting or a relatively small sample size. This unusual technique offering new possibilities for nucleation of gold nanoparticles was compared with conventional melting.

The goal was to add low concentrations of gold into studied glasses and investigate the influence of chemical composition as well as additional heat treatment and used technology on size, shape, and distribution of Au nanoparticles in the glass matrix. First, series of yttrium aluminosilicate glasses (YAS) was prepared. System  $Y_2O_3$ -Al $_2O_3$ -Si $O_2$  was chosen because glasses in this system have advantageous mechanical and optical properties such as high hardness and refractive indices. The properties, composition and structure of the glass were studied by DSC, XRF, XRD. The presence and properties of gold nanoparticles were determined by optical absorption, scanning and transmission electron microscopy. Our experiments with YAS glasses showed that the key factor for melting glasses with gold is the temperature used during the ADL melting process. That was why we shifted our focus to lithium disilicate glass (Li $_2$ O'2SiO $_2$ ) which was chosen because of its low melting temperature. Finally, a series of lithium yttrium aluminosilicate glasses (LYAS) with varying composition and gold content was prepared with the intention to combine the advantageous properties of the two previous systems. The relationship between the optical absorption as well colour of the glass and the shape and distribution of the nanoparticles was studied and discussed.

<sup>&</sup>lt;sup>1</sup>Department of Inorganic Chemistry, University of Chemistry and Technology, Technická 5, 166 28 Prague 6, Czech Republic

<sup>&</sup>lt;sup>2</sup>Conditions Extrêmes et Matériaux : Haute Température et Irradiation (CEMHTI), CNRS UPR 3079, 1D Avenue de la Recherche Scientifique, 45071 Orléans Cedex 2, France

# Highly nonstoichiometric $Tb_2Y_{0.1-1}Al_5O_{12}$ : Ce single crystals with modified microstructure, defect concentration, luminescence, and scintillation properties

<u>Karol Bartosiewicz</u><sup>1</sup>, Masao Yoshino<sup>2</sup>, Takahiko Horiai<sup>2</sup>, Marcin Witkowski<sup>3</sup>, Damian Szymanski<sup>4</sup>, Shunsuke Kurosawa<sup>2,5,6,7</sup>, and Akira Yoshikawa<sup>2,6</sup>

<sup>1</sup>Faculty of Physics of Kazimierz Wielki University, Powstańców Wielkopolskich 2, 85-090 Bydgoszcz, Poland

<sup>2</sup>New Industry Creation Hatchery Center, Tohoku University, Sendai, Miyagi, Japan

<sup>3</sup>Faculty of Physics, Nicolaus Copernicus University, Toruń, Poland

<sup>4</sup>Institute of Low Temperature and Structure Research, Polish Academy of Sciences, Wrocław,

Poland

<sup>5</sup>Institute for Materials Research, Tohoku University, Sendai, Miyagi, Japan <sup>6</sup>Institute of Laser Engineering, Osaka University, Osaka, Japan <sup>7</sup>Faculty of Science, Yamagata University, Yamagata, Japan

The  $Ce^{3+}$  doped  $Y_3Al_5O_{12}$  (YAG:Ce) single crystal is a member of the family of high-performance complex oxide scintillators. Ce<sup>3+</sup> centers exhibit high quantum efficiency and fast response with a decay time of approximately 50 ns in the 520 nm emission band [1]. However, the YAG host lattice contains electron traps associated with antisite defects and oxygen vacancies, which considerably reduces the yield of scintillation light and decelerate the kinetics of scintillation decay. Increasing the concentration of Ce<sup>3+</sup> ions to improve the capture of electron-hole pairs is not feasible because energy transfer between Ce<sup>3+</sup> ions can reduce the light output. The improvement of scintillation parameters can be achieved by enhancing energy transfer from the host lattice to the activator. Introducing Tb atoms to the host lattice can efficiently transfer excitation energy towards Ce<sup>3+</sup> ions [2]. Previous reports have revealed that an excess of  $RE_2O_3$  increases the concentration of  $RE_{Al}$  antisite defects (ADs). Therefore, in order to reduce the concentration of RE<sub>Al</sub> ADs, strong non-stoichiometry was introduced to  $Ce^{3+}$ -doped  $Tb_2Y_1Al_5O_{12}$  single crystals. This research investigates the crystal growth of both stoichiometric Tb<sub>2</sub>Y<sub>1</sub>Al<sub>5</sub>O<sub>12</sub>:Ce and non-stoichiometric Ce<sup>3+</sup>-doped Tb<sub>2</sub>Y<sub>0.1</sub>Al<sub>5</sub>O<sub>12</sub> single crystals using the  $\mu$ -PD method. The study aims to explore the influence of non-stoichiometry on various aspects, including crystal growth, microstructure distortion, defect concentration as well as luminescence and scintillation properties. To analyze these effects, XRD, SEM-EDS, thermally stimulated luminescence, photoluminescence, and scintillation properties are utilized.

- [1] M. Nikl, et al., Prog. Cryst. Growth Charact. Mater. 59 (2013) 47-72.
- [2] K. Bartosiewicz, et al., Phys. Status Solidi RRL 2020, 2000327.

#### Heat source models for numerical simulation of laser welding processes

#### Mária Behúlová and Eva Babalová

Slovak University of Technology in Bratislava, Faculty of Materials Science and Technology in Trnava, Ulica Jána Bottu č. 2781/25, 917 24 Trnava, Slovakia

In recent decades, numerical modeling and computer simulation have become an integral part of the design, analysis and optimization of fusion welding processes, including laser welding [1-2]. In general, laser welding processes involve the interaction of multiple physical phenomena, such as thermal, fluid, metallurgical, chemical, mechanical, and diffusion effects, which makes the development of a simulation model difficult and complex. In addition to the geometric characteristics of the parts to be welded, their material properties must be specified in a wide temperature range, as well as the conditions for heat removal to the environment or shielding gas. One of the most complex tasks in the preparation of a simulation model of the laser welding process consists in the selection of an appropriate heat source model to accurately determine the heat input to the weld [3-6]. Very important is also the process of experimental verification and validation of the developed simulation models [7].

In this paper, a short examination of significant 3D mathematical heat source models for numerical simulation of laser welding is provided. Numerical analysis of laser welding of aluminum sheets is accoplished using selected 3D heat source models with the support of the ANSYS code. The achieved results are compared and discussed with respect to the specific parameters that characterize individual heat source models.

- [1] L E Lindgren, J Therm Stresses 24 (2001) 141.
- [2] A P Mackwood, Opt Laser Technol 372005 (2005) 99.
- [3] M Dal and R Fabbro, Opt Laser Technol 78 (2016) 2.
- [4] J Svenungsson, I Choquet and A F H Kaplan, Physics Procedia 78 (2015) 182.
- [5] T Kik, Materials 13 (2020) 2653. https://doi.org/10.3390/ma13112653
- [6] R M Farias, P R F Teixeira and L O Vilarinho, Int J Therm Sci 179 (2022) 107593.
- [7] M Courtois et al J Phys D: Appl Phys 49 (2016) 155503.

## Point defects creation and their influence on luminescent properties of 0D, 1D, 2D and 3D materials

<u>Maksym Buryi</u><sup>1</sup>, Vladimir Babin<sup>1</sup>, František Hájek<sup>1</sup>, Tomáš Hubáček <sup>1</sup>, Anna Artemenko<sup>1</sup>, Zdeněk Remeš<sup>1</sup>, and Júlia Mičová<sup>2</sup>

<sup>1</sup>FZU - Institute of Physics of the Czech Academy of Sciences, Cukrovarnická 10/112, Prague, Czechia

<sup>2</sup>Institute of Chemistry SAS, Dúbravská cesta 9, 845 38, Bratislava, Slovakia

The scintillators are the transformers of high energy incident radiation to low energy photons. In particular, they are used as radiation detectors in positron emission tomography (PET) or computed tomography (CT). Improved sensitivity and timing characteristics of the scintillating detector result in the decreased radiation dose delivered to a patient. Zinc oxide (ZnO), gallium nitride (GaN), cesium lead bromide (CsPbBr $_3$ , CPB) and cesium copper iodide (Cs $_3$ Cu $_2$ I $_5$ , CCI) exhibited great potential as the detector materials in PET and CT applications.

ZnO has excellent physical properties. It is cheap and can be easily grown as a nanopowder, in the form of free-standing nanorods or nanorods deposited onto a substrate.

GaN has scintillating properties very similar to those of the ZnO. It can be synthesized in the variety of forms as well. One of the forms is indium doped GaN (InGaN) multiple quantum wells (MQW) grown on a GaN layer - a kind of thin film multilayer structure, where the thickness of a single layer is about 2-3 nm.

CPB grown as larger nanoparticles or quantum dots has prominent timing characteristics, large light and quantum yields.

It is known that the 0D polyanionic inorganic networks like CCI:Tl(In) support the exciton emission reaching very high photoluminescence quantum efficiency (PLQE) of about 80-90%. Moreover, the high light yield (LY) of 50000-90000 ph/MeV [1,2] can be reached there. Remarkably, the growth of the undoped and Tl doped  $Cs_3Cu_2I_5$  in the form of thin film exhibited scintillation efficiency at the level of one third of that of CsI:Tl whereas the afterglow was by about one order of magnitude weaker as compared to the CsI:Tl [3].

All of these materials suffer from intrinsic and extrinsic defects participating in luminescence processes and charge trapping phenomena affecting LY and PLQE. Therefore, knowing the defects types is very important. This is the aim of the present work.

- [1] S. Cheng et al., Advanced Optical Materials 9 (2021) 2100460.
- [2] Q. Wang et al., Advanced Optical Materials 10 (2022) 2200304.
- [3] Q. Wang, M. Nikl, S. Cheng, G. Ren, Y. Wu, Physica Status Solidi (RRL) Rapid Research Letters 15 (2021) 2100422.

#### **Extreme Large 2D and 3D Nanoscale Application**

**Antonio Casares** 

Carl Zeiss Microscopy, Carl Zeiss Str. 22, 73447 Oberkochen, Germany

Modern microscopy labs are typically outfitted with a suite of instruments, capable of capturing data across a range of length scales in 2D- and 3D, from the centimeters to the sub-nanometers. These imaging instruments are often complimented by analytical techniques, such as spectroscopic chemical characterization platforms or mass spectrometry and are designed to produce a comprehensive depiction of the material under investigation. Recently, a novel multi-beam SEM (MSEM) technology for imaging of large sample areas has been developed by ZEISS. The MultiSEM family features 61 or even 91 electron beams scanning in parallel, resulting in an imaging throughput of up to 2 TeraPixels per hour (s. ref.) is now achievable, therefore enabling extremely large-scale imaging experiments in 2D and 3D. Here, we present a unique advancement enabling correlative microscopy, which uses a centralized software platform to pull together data from light-, electron-, Ion-, and X-Ray Microscopy (XRM). Beyond just correlating the various datasets, the approach allows data from one technique to be used to drive the hardware in another technique, facilitating easy transfer of information between the suite of available microscopes and the operator. The presentation will give an overview of the current state of the technology, its potential application space and the challenges in data handling imposed by the enormously increased data rate.

[1] K. Crosby, A. Eberle, D. Zeidler, Multi-beam SEM Technology for High Throughput Imaging. MRS Advances, 1 (2016) (26):1915–1920.

#### Study of phase equilibria in Al-Co and Pd-Co systems

<u>Ivona Černičková</u><sup>1</sup>, Libor Ďuriška<sup>1</sup>, Peter Švec sr.<sup>2</sup>, and Jozef Janovec<sup>1</sup>

<sup>1</sup>Faculty of Materials Science and Technology in Trnava, Slovak University of Technology in Bratislava, Jána Bottu 2781/25, Trnava 91724, Slovakia

System Al-Pd-Co contains not only classical crystalline phases with simple unit cells, but also structurally complex phases with large unit cells, inclusive of quasicrystalline approximant  $\varepsilon_n$ . Experimental partial isothermal sections of the Al-Pd-Co phase diagram at 700°C [1] 790 [2], 850°C [3], 940, 1000 [2], 1020 [4], 1035 [5] and 1050°C [2] have been published so far. Experimental studies and thermodynamic modeling of Al-Pd binary system were done previously [6,7]. The aim of this work is to study the phase equilibria in Al-Co and Pd-Co binaries. Thermodynamic databases of Al-Co and Pd-Co were created based on literature. The calculations were performed by means of the CALPHAD method using the Thermo-Calc software. A thermodynamic description of Al-Pd-Co was created by extrapolation of binary systems. A novel thermodynamic description of U and C phase was proposed based on ternary thermodynamic model. The (Co),  $\beta$ -AlCo, Al<sub>5</sub>Co<sub>2</sub>, Al<sub>9</sub>Co<sub>2</sub>, Al<sub>13</sub>Co<sub>4</sub> and (Al) phases belong to the Al-Co system. (Co) and (Pd) solid solutions belong to Pd-Co system. Structurally complex phases of  $\varepsilon$ -family and Al<sub>13</sub>Co<sub>4</sub>-family were experimentally observed. In investigation, scanning electron microscopy, energy dispersive X-ray spectroscopy, transmission electron microscopy and X-ray diffraction were used. Experimental results were then compared to calculated phase diagrams.

- [1] I. Černičková, R. Čička, P. Švec, D. Janičkovič, P. Priputen, and J. Janovec, in A Study of Phase Equilibria in the Al-Pd-Co System at 700 °C, edited by S. Schmid, R. L. Withers, and R. Lifshitz, Aperiodic Crystals (Springer-Verlag, Berlin, 2013), Chap. 18.
- [2] M. Yurechko, B. Grushko, T. Velikanova, and K. Urban, J. Alloys Compd. 337 (2002) 172.
- [3] I. Černičková, L. Ďuriška, P. Priputen, D. Janičkovič, and J. Janovec, J. Phase Equilib. Diffus. 37 (2016) 301.
- [4] L. Ďuriška, I. Černičková, P. Priputen, and J. Janovec, J. Phase Equilib. Diffus. 40 (2019) 45.
- [5] I. Černičková, L. Ďuriška, P. Švec, P. Švec Sr, M. Mihalkovič, P. Priputen, P. Šulhánek, and J. Janovec, J. Alloys Compd. 896 (2021) 162898.
- [6] L. Ďuriška, I. Černičková, R. Čička, and J. Janovec, J. Phys. Conf. Ser. 809 (2017) 012008.
- [7] M. Yurechko, A. Fattah, T. Velikanova, and B. Grushko, J. Alloys Compd. 329 (2001) 173.

<sup>&</sup>lt;sup>2</sup>Institute of Physics, Slovak Academy of Sciences, Dúbravská cesta 9, Bratislava 84511, Slovakia

# Analysis of phase transformations in Fe - 1.1C - 0.9Si – 0.4Mn – 8.3Cr – 2.1 Mo – 0.5V steel using dilatometry and computational thermodynamics

Roman Čička and Jozef Krajčovič

Institute of Materials, Faculty of Materials Science and Technology, Slovak University of Technology, Jána Bottu 25, Trnava, 917 24, Slovakia

Steels represent the important class of materials with wide range of properties, depending on their composition and processing. Understanding the phase transformations during heating and cooling and the influence of alloying elements on the kinetics of these phase transformations is essential for improving the properties of steels [1]. In this work the phase transformations in Fe - 1.1 C - 0.9 Si - 0.4 Mn - 8.3 Cr - 2.1 Mo - 0.5 V tool steel are described using dilatometry and computational thermodynamics. NETZSCH DIL 402 C dilatometer, Thermo-Calc [2] and JMatPro [3] software were used. In dilatometry experiments the constant heating rate 5K/min and different cooling rates (1 - 15) K/min were used, in temperature range (30 - 1100)  $^{\circ}$ C. The results emphasize the importance of computational thermodynamics in interpreting and understanding the experimental data related to phase transformations.

- [1] E. Pereloma, D.V. Edmonds: Phase transformations in steels. Volume 1: Fundamentals and diffusion-controlled transformations. Woodhead Publishing Limited, 2012.
- [2] https://thermocalc.com
- [3] https://www.sentesoftware.co.uk/jmatpro

#### Ion Beam Analysis including ToF ERDA of complex composition layers

Jozef Dobrovodský¹, Dušan Vaňa¹, Matúš Beňo¹, František Lofaj², and Robert Riedlmajer¹

<sup>1</sup>Slovak University of Technology in Bratislava, Faculty of Materials Science and Technology in Trnava, Jána Bottu č. 2781/25, 917 24 Trnava, Slovakia

<sup>2</sup>Institute of Materials Research of the Slovak Academy of Sciences, Watsonova 47, 04001 Košice, Slovakia

Several analytical methods based on different physical principles are used to determine the depth distribution of elements in the surface layers of materials. These are, for example, XPS, AES, EDX, SIMS, ICP-MS, Raman spectroscopy, etc., while each of the methods has its own specifics, advantages and disadvantages. When developing new materials such as radiation, high temperature and corrosion resistant, hard coatings, next-generation electrode materials for various applications in electrochemistry, but also in semiconductors field, etc., it is indispensable the knowledge of detailed elemental composition from surface to a depth of several micrometers. For the quantitative determination of elemental depth profile of such samples, also established quantitative IBA (Ion Beam Analysis) methods such as RBS, EBS, NRA, PIXE and ERDA are applicable, the advantage of which is that they are considered to be absolute and non-destructive. Each of these methods is advantageously used to analyze a certain range of elements, sometimes depending on the combination of other elements present.

If the analysis of thin layers with a complex composition is required, e.g. with a content ranging from heavy elements such as W, through rare earths such as Ta, Hf to Ti, with a content of light elements ranging from Si through Mg, N, B to H, it is already quite a challenging task. In such a case, it is necessary to use a combination of several, many times even all of the abovementioned IBA methods. Then iterative evaluation of separate IBA data is necessary, which is a more demanding and time-consuming activity, but the output is depth profiles of layers with a complex elemental composition with a thickness from few nanometers up to 3 micrometers.

The recently commissioned ToF-ERDA measurement IBA system significantly expands the analytical possibilities of thin layers up to micrometer depth. Using the primary analyzing 50 MeV Au beam, the depth profiles of all elements from W to H can be obtained within a single measurement. On the examples of multi-elemental samples analysis, the gained results, difficulty of measurement and evaluation of ToF-ERDA on the one hand, and of the combination of the other above-mentioned IBA methods are compared and evaluated.

# A measuring of the sound absorption coefficient of structured materials produced by 3D printing

Rastislav Ďuriš and Eva Labašová

Slovak University of Technology, Faculty of Materials Science and Technology, ul. Jána Bottu 25, Trnava, 917 24, Slovakia

Currently, industry is increasingly using 3D printing for the production of prototypes or small-lot products. 3D printing is significantly cheaper than other traditional production methods, saves material, time and money. The principle of operation of 3D printing is based on the systematic, step-by-step pre-set stacking of individual layers on top of each other, which creates the final product.

The aim of the contribution is to present the possibilities of using 3D FDM printing in the production of acoustic dampening materials designed to have the desired absorption properties. A simple circular samples with a diameter of 89 mm and three different thicknesses of 14, 20, 28 mm were produced using this method. In addition to the thickness, the internal structure of the samples was also changed. The prepared samples were tested using an impedance tube (1). The impedance tube made by us and the measurement of the acoustic properties of the test samples using it took place in accordance with the standards ASTM E 1050 (2) and ISO 10534-2 (3). A two-microphone method based on the calculation of transfer functions (2) was used to measure the absorption coefficient of the designed sample structures. The microphones were connected to the measuring center and to the PULSE system. PULSE Labshop software was used to estimate the frequency dependence of sound absorption coefficients.

The paper analyzes the experimentally obtained values of the absorption coefficient for different structures and thicknesses of samples produced by 3D printing. The measurements were evaluated in the range of frequencies from 100 Hz to 1600 Hz. White noise was used as the sound source.

- [1] ĎURIŠ, Rastislav LABAŠOVÁ, Eva. The design of an impedance tube and testing of sound absorption coefficient of selected materials. In IOP Conference Series: Materials Science and Engineering. Vol. 1050, DMSRE, 07.-11. september 2020, Pavlov, ČR (2021), s.1-10. ISSN 1757-8981 (2021). V databáze: DOI: 10.1088/1757-899X/1050/1/01200; SCOPUS: 2-s2.0-85101685797.
- [2] ASTM E 1050 1998 Standard test method for impedance and absorption of acoustical material using a tube, Two microphones and a digital frequency analysis system.
- [3] ISO 10534-2 1998 Acoustics Determination of sound absorption coefficient and impedance in impedance tubes Part 2: transfer-function method.

### Structural, thermal and mechanical properties of gallium-enriched SAC lead-free solders

<u>Libor Ďuriška</u>, Ivona Černičková, Marián Drienovský, Roman Moravčík, Ladislav Dobrovodský, and Roman Čička

Faculty of Materials Science and Technology in Trnava, Slovak University of Technology in Bratislava, Jána Bottu 2781/25, Trnava 91724, Slovakia

The most promising lead-free solders are SnAgCu (SAC) [1,2]. Although a lot of work has been done in this area in recent years, properties of these solders have not yet been fully optimized, especially in relation to previously used lead-based solders [3]. In order to improve the properties of lead-free solders, additional alloying elements can be introduced [4]. The aim of this work is to study the effect of Ga addition on structural, thermal and mechanical properties of SAC. In the experimental investigation, scanning electron microscopy, energy-dispersive X-ray spectroscopy, X-ray diffraction, differential scanning calorimetry and Vickers hardness testing were used. It was found that the microstructure of the SAC solder contains three types of phases - (Sn), Ag-rich and Cu-rich. If gallium is added, the phase composition and morphology starts to differ. Besides that, the melting point decreases. The Vickers hardness was found to increase with increasing Ga content. Experimental results were then compared to calculations obtained using the Thermo-Calc software.

- [1] K. S. Kim, S. H. Huh, and K. Suganuma, Microelectron. Reliab. 43 (2003) 259.
- [2] W. R. Osório, L. C. Peixoto, L. R. Garcia, N. Mangelinck-Noël, and A. Garcia, J. Alloys Compd. 572 (2013) 97.
- [3] M. A. Fazal, N. K. Liyana, Saeed Rubaiee, and A. Anas, Measurement 134 (2019) 897.
- [4] Q. K. Zhang, W. M. Long, X. Q. Yu, Y. Y. Pei, and P. X. Qiao, J. Alloys Compd. 622 (2015) 973.

#### **Analysis of Biocompatible Metallic Materials used in Medicine**

Žaneta Gerhátová, Jozef Paták, Paulína Babincová, Mária Hudáková, and Marián Palcut

Faculty of Materials Science and Technology in Trnava, Slovak University of Tech, Jána Bottu 25, Trnava, Slovakia

The paper presents the results of the analysis of two biocompatible materials, Kirschner wires of different thicknesses. Scanning electron microscopy and light microscopy were used to document the microstructure. Before observation, the wires were prepared by a standard metallographic procedure (grinding and polishing) followed by electrolytic etching. The chemical composition was determined by studying the wires using quantitative energy-dispersive X-ray spectrometry. It has been found that the chemical composition of the materials corresponds to Cr-Ni stainless steel. In the thick Kirschner wire (sample no. 1) a deformed microstructure after drawing was observed. Sample no. 2 (thin Kirschner wire), on the other hand, consisted of polyhedral austenitic grains, which were formed after recrystallization annealing. Furthermore, isolated microparticles were observed and assigned to titanium nitride. A Vickers hardness test was also performed on the samples. It has been found that the microhardness of sample no. 1 was 428.8 HV 0.5. The average microhardness of sample no. 2 was 213.4 HV 0.5. It can be concluded that recrystallization annealing decreases the hardness of the material.

**Keywords:** biocompatible material, austenitic stainless steel, Kirschner wire, Vickers hardness test.

#### Basic study of lithium strontium borates as thermal neutron scintillators

<u>Jan Havlíček</u><sup>1</sup>, Kateřina Rubešová<sup>1</sup>, Vít Jakeš<sup>1</sup>, Romana Kučerková<sup>2</sup>, Alena Beitlerová<sup>2</sup>, and Martin Nikl<sup>2</sup>

A special group of luminescence materials are scintillators for thermal neutron detection. Due to different mechanisms of neutron interaction with matter (contrary to e.g. electrons or gamma photons), a different approach has to be utilized — the high content of atoms with the sufficient absorption cross-section toward neutrons and lower material density are needed. This contribution pursues a basic study of LiSrBO<sub>3</sub> and LiSr<sub>4</sub>(BO<sub>3</sub>)<sub>3</sub> doped with cerium or europium &mdash; materials promising as thermal neutron scintillators. These borates exhibit promising properties such as the high content of lithium and boron, suitable density, and proper environment for luminescent ions. Radioluminescence of these ceramic borates doped with cerium and europium was examined and promising samples were further characterized by photoluminescence spectroscopy and radioluminescence and photoluminescence kinetics measurement. The most promising material &mdash; LiSr<sub>4</sub>(BO<sub>3</sub>)<sub>3</sub>:Ce was further characterized in a form of translucent ceramics prepared by a SPS sintering.

<sup>&</sup>lt;sup>1</sup>Department of Inorganic Chemistry, University of Chemistry and Technology, Technická 5, Praque 6, 166 28, Czechia

<sup>&</sup>lt;sup>2</sup>Institute of Physics of the Czech Academy of Sciences, Cukrovarnická 10, 162 00, Prague 6, Czechia

#### Crystal growth and optical characterization of Ce-doped mixed rare-earth sesquioxide single crystals for scintillator applications

<u>Takahiko Horiai</u><sup>1,2</sup>, Yuui Yokota<sup>1,2</sup>, Masao Yoshino<sup>1,2</sup>, and Akira Yoshikawa<sup>1,2</sup>

<sup>1</sup>New Industry Creation Hatchery Center, Tohoku University, 6-6-10 Aoba, Sendai, Japan <sup>2</sup>Institute for Materials Research, Tohoku University, 2-1-1 Katahira, Sendai, Japan

Scintillation materials, which can convert a high energy photon such as gamma-rays and X-rays into low-energy photons such as UV and visible light, are widely used as radiation detectors when combined with photodetectors. Focusing on oxide scintillators, which are relatively high density and chemically stable, single crystals have been grown from melts using the Czochralski technique and/or the micro-pulling-down ( $\mu$ -PD) method with metal crucible [1]. For the development of novel oxide scintillator materials, we focused on mixed rare-earth sesquioxide with melting points between 2,100 and 2,230°C, which is near the softening point of the iridium used as a crucible material [2]. Thus, in this study, we investigated the crystal growth method combining the  $\mu$ -PD method and a tungsten crucible for growing Ce-doped YScO<sub>3</sub> single crystals and evaluated their optical properties.

As starting materials, commercial oxide powders  $(Y_2O_3, CeO_2)$  with purities of over 99.99% and  $Sc_2O_3$  powder with purity of over 99.9% were used. After weighing according to  $(Ce_x Y_{1-x})ScO_3$   $(0.2 \le x \le 3.0)$ , the powders were formed into pellets by a hydraulic press. The pellets were sintered at  $1700^{\circ}C$  for 24 hours under air atmosphere. After the sintered compact was crushed into powder, the powder was filled into a tungsten crucible and crystals were grown at a pulling-down rate of 0.03 mm/min. To prevent oxidation of the tungsten crucible during crystal growth, deoxygenated stabilized zirconia was used for insulation [3].

As a result of crystal growth, we succeeded in growing transparent Ce-doped YScO $_3$  crystals. The grown crystals showed orange coloration, thus we measured the transmittance and found broad absorption in the wavelength range of 400-600 nm. Since this absorption was considered to be caused by oxygen vacancies generated during crystal growth, we annealed the grown crystals at 1200°C for 12 hours under an atmospheric atmosphere and obtained transparent crystals. From the results of the powder X-ray diffraction analysis, the crystalline system and the space group were identified cubic and Ia-3, respectively. However, the crystals with Ce concentration of 1% or more contained small diffraction peaks around 2  $\vartheta$  of 31° and 32°, which originated from different phases.

- [1] A. Yoshikawa, et al., Opt. Mater. 30 (2007) 6.
- [2] R. Uecker, et al., J. Cryst. Growth, 310 (2008) 2649.
- [3] T. Suda, T. Horiai, A. Yoshikawa, et al., J. Cryst. Growth, 575 (2021) 126357.

### Structure and properties of Ag<sub>2</sub>O-GeO<sub>2</sub>-P<sub>2</sub>O<sub>5</sub> glasses

Tomáš Hostinský, Petr Mošner, and Ladislav Koudelka

Department of General and Inorganic Chemistry, Faculty of Chemical Technology, University of Pardubice, 532 10 Pardubice, Czech Republic

Phosphate glasses of the  $Ag_2O-GeO_2-P_2O_5$  were studied in two compositional series (50-x) $Ag_2O-xGeO_2-50P_2O_5$  with 0-50 mol%  $GeO_2$  and  $50Ag_2O-xGeO_2-(50-x)P_2O_5$  with 0-20 mol%  $GeO_2$ . Basic physical properties were determined, and thermal properties studied by differential thermal analysis, thermomechanical analysis, and hot-stage microscopy. The glass structure was investigated using Raman spectroscopy and  $^{31}P$  MAS NMR by both 1D and 2D techniques. The electrical properties of the glasses were obtained by using impedance spectroscopy.

In both glass series glass transition temperature increases with GeO2 additions and all glasses containing GeO<sub>2</sub> crystallizes in temperature range 500-750 °C. The dependence of the coefficient of thermal expansion in both cases sharply decreased with the addition of  $GeO_2$ , which is a typical phenomenon when  $T_q$  increases, and indicates the strengthening of the structural network of the glass due to the increase in the occurrence of Ge-O bonds. <sup>31</sup>P MAS NMR spectra of (50-x)Ag<sub>2</sub>O-xGeO<sub>2</sub>-50P<sub>2</sub>O<sub>5</sub> series were dominated by one major resonance which shifts to more negative values with increase of GeO<sub>2</sub> content. Position and the shift of the peak indicates that network of the glass is mainly built from  $Q^2$  structural units. By using 2D  $^{31}\text{P}$ INADEQUATE sequence was confirmed that phosphate chains are gradually shortened due to the formation of Ge-O-P bonds. <sup>31</sup>P MAS NMR spectra of 50Ag<sub>2</sub>O-xGeO<sub>2</sub>-(50-x)P<sub>2</sub>O<sub>5</sub> consist of multiple peaks that mainly belong to structural units Q<sup>1</sup> and Q<sup>2</sup>. Spectra of this series are also influenced by hygroscopicity of the glasses. Raman spectra of the glasses includes dominant vibrational band in the region  $1000-1300 \text{ cm}^{-1}$ , changes in this region reveals transformation of phosphate glass network. Another dominant vibrational bands can be found in the region 500-800 cm<sup>-1</sup>. This region reflects evolution of P-O-P connections to P-O-Ge and Ge-O-Ge connections through the series.

# The influence of structure, sensitization and corrosion on the fatigue properties of AISI 304 austenitic steel

Silvia Hudecová, <u>Milan Uhríčik</u>, Peter Palček, Viera Zatkalíková, Lenka Markovičová, Martin Mikolajčík, Veronika Chvalníková, and Martin Slezák

University of Žilina, Department of Materials Engineering, Univerzitná 8125/1, Žilina, Slovakia

Austenitic stainless steels are widely used biomaterials owing to their high biocompatibility and corrosion resistance. Their current study mostly aims to further improve their mechanical properties, wear and local corrosion resistance [1]. The protective passive film on the stainless steel surface ensures high resistance to the uniform corrosion in common oxidation environments, but under special conditions local corrosion forms can be initiated [2].

The article will be focused on examining and comparing the influence of structure, sensitization and corrosion on the fatigue properties of austenitic stainless steel. The methodology of the experiment includes fatigue tests of samples attacked by intercrystalline corrosion. Therefore, the test samples were subjected to heat treatment for sensitization. Then these samples were subjected to long-term exposure in an aggressive corrosion solution.

Experiments deal with microstructural material analysis, fractographic analysis, mechanical and fatigue tests. The microstructure of the testing sample was examined using a light microscope (LM) ZEISS Neophot 32. A Vickers hardness test was performed on a Zwick/Roell ZHV  $\mu$ -A test apparatus. Fatigue properties of austenitic steel were tested by three-point bending cyclic loading. Fatigue tests have been carried out on testing machine ZWICK/ROELL Amsler 150 HFP 5100. The fracture surface of the testing sample was examined using a scanning electron microscope (SEM) TESCAN Vega II LMU, where samples were observed on various stages of the fatigue process, their characteristics and differences of fracture surfaces.

The aim of this work is to analyze stainless austenitic steel after heat treatment (sensitization) and exposure in a corrosive environment, by comparing and evaluating the results of fatigue tests and fracture surface fractography.

- [1] V. Zatkalíková, J. Halanda, D. Vaňa, M. Uhríčik, L. Markovičová, M. Štrbák, and L. Kuchariková, Materials 14 (2021) 6790.
- [2] T. Lipiňski, Prod. Eng. Arch. 27 (2021) 108.

# Y-stabilized hafnia as a potential scintillating material for ionizing radiation detection

<u>Vít Jakeš</u><sup>1</sup>, Kateřina Rubešová<sup>1</sup>, Tomáš Thoř<sup>1</sup>, Jiří Prikner<sup>1</sup>, Christo Guguschev<sup>2</sup>, Romana Kučerková<sup>3</sup>, Jan Pejchal<sup>3</sup>, and Martin Nikl<sup>3</sup>

<sup>1</sup>University of Chemistry and Technology, Technická 5, Praha 6, Czechia <sup>2</sup>Leibnitz-Institut für Kristallzüchtung, Max-Born-Strasse 2, 12489 Berlin, Germany <sup>3</sup>Institute of Physics, Academy of Sciences of the Czech Republic, Cukrovarnická 10/112, 16200 Praha 6, Czechia

Beside the improvement in performance of already applied scintillators, the research focuses on finding new scintillating materials and further characterizing less known materials. One of the potential, yet not fully investigated, materials is hafnia (HfO $_2$ ). Due to its high density it can be employed as a heavy matrix with high stopping power and therefore suitable for high energy physics, for example. Hafnia has three polymorphs. The monoclinic phase is the low-temperature polymorph that transforms into the tetragonal phase at 1800  $^{\circ}$ C and, upon further heating, the cubic phase is obtained at 2630  $^{\circ}$ C; the band-gap of the cubic phase was reported to be around 6.03 eV. Based on the similarity with zirconia and the stabilization of its cubic structure at lower temperatures by yttria doping, the stabilization of the hafnia cubic phase by Y doping was reported. The amount of Y necessary for the stabilization of the cubic phase depends on the preparation method and may vary from 6 to 24 % of Y. Depending also on the synthesis method, ferroelectric orthorhombic phase may be formed if not enough yttrium is doped.

 $\rm HfO_2$  was studied as a host for selected rare earths photoluminescence; however, Ce-doped Y-stabilized single crystals have never been studied for either scintillation applications or any other purposes. To close this knowledge gap, the purpose of this work was to prepare sintered ceramic rods that will be later used in Optical Floating Zone (OFZ) processing of single crystals of Y,Ce: $\rm HfO_2$  and characterize the luminescence in this material. Due to the high melting point of  $\rm HfO_2$ , OFZ method is perspective for research of such a material. Single crystals of the cubic  $\rm HfO_2$  stabilized by 20 % Y were recently prepared for ferroelectricity studies by this method. Nevertheless, our goal is to study the relation between the content of cerium and yttrium in the hafnia matrix, and scintillation properties.

First, feed and seed ceramic rods were prepared. The precursors to our samples of yttria-stabilized  $HfO_2$  (nominal composition:  $Y_{y-x}Ce_xHf_{2-x}O_{1.9}$ ; y=0.11, 0.12, 0.2 and x=0, 0.01, 0.001) were prepared by a solid state reaction. The powders were then pressed isostatically into rods which were subsequently sintered at 1650 °C for prolonged time. The phase composition and microstructure of these rods were characterized by XRD and SEM. Cross sections of these samples were then post-annealed in inert ( $N_2$ ) or reducing ( $SH_2/SAr$ ) atmospheres and radioluminescence was measured to evaluate the luminescence of cerium. Prepared rods were subsequently used for the OFZ growth of single crystals which are now being characterized.

#### Advances in hydroxyapatite dosimetry: New trends

<u>David John</u><sup>1,2,3</sup>, Maksym Buryi<sup>1,2</sup>, Kateřina Pachnerová Brabcová<sup>3</sup>, and Ivo Světlík<sup>3</sup>

<sup>1</sup>FZU - Institute of Physics of the Czech Academy of Sciences, Cukrovarnická 10, 16200 Praha 6, Czechia

<sup>2</sup>Faculty of Nuclear Sciences and Physical Engineering, Břehová 78/7, 11000 Praha 1, Czechia

<sup>3</sup>Nuclear Physics Institute of the Czech Academy of Sciences, Husinec - Řež, čp. 130, 25068 Řež, Czechia

Hydroxyapatite is a major component of all organic solid tissues and has a wide range of applications. Biohydroxyapatite (bHAP) dosimetry is used to determine doses from artificial radiation exposure or archaeology to determine the age of remains. EPR dosimetry of dental enamel is considered the gold standard of retrospective dosimetry. Despite decades of research, it has not yet been possible to elucidate the origin, exact number or parameters of all signals in the complex EPR spectrum of bHAP. At room temperature, these signals overlap and saturate at low temperatures, so the applicability of the method has been limited to cases of large accumulated dose in bHAP. In this work we have attempted to examine the validity of this limitation using the advances and sensitivity of current and modern EPR measurement equipment.

# Influence the effect of balancing the grinding set on the accuracy and roughness of the machined surface

František Jurina, Tomáš Vopát, Marek Vozár, and Boris Pätoprstý

MTF STU, Ulica Jána Bottu č. 2781/25, Trnava, Slovakia

The article examines the effect of balancing the grinding wheel set on the accuracy and roughness of the machined surface during the production of cutting tools. Screw drills with a diameter of 12 mm were manufactured as well as samples in the shape of a recess with a width of 20 mm and a diameter of 18 mm. The workpiece material was sintered carbide (WC+Co). Properly balanced and unbalanced sets of cubic boron nitride (CBN) and synthetic diamond grinding wheels were used in the production of the tools and samples. A WZS 60 Reinecker tool grinder was used as the machine. The parameters of surface roughness and dimensional accuracy were measured in the experiment. Surface roughness was evaluated on a Zeiss Surfcom 5000 shape and contour measuring machine. Dimensional accuracy measurement was performed on an optical measuring machine Zoller Genius 3. In terms of dimensional accuracy, tools and samples produced by wheel balancing to a lower level of balance quality G show greater dimensional inaccuracy than tools and samples produced by wheel sets that were balanced to a higher quality level of balance G. From the point of view of evaluating the surface roughness, the results were not clear, but the tools and samples produced by CBN grinding wheels showed better surface roughness, regardless of the quality level of balance G.

# Development and material design of structured scintillators for high resolution radiation imaging and thermal neutron detection

<u>Kei Kamada</u><sup>1,2</sup>, Rei Sasaki<sup>1</sup>, Naoko Kutsuzawa<sup>2</sup>, Masao Yoshino<sup>1,2</sup>, Yuji Shirakami<sup>2</sup>, Yoshiyuki Usuki<sup>2</sup>, Takahiko Horiai<sup>1,2</sup>, and Akira Yoshikawa<sup>1,2</sup>

<sup>1</sup>Tohoku Univ., 2-1-1 Katahira, Sendai, Miyagi, 980-8579, Japan <sup>2</sup>C&A corporation. 1-16-23, Ichiban-tyo, Aoba-ku, Sendai, Miyagi, 980-0811, Japan

In this talk, our research on functional composites with considering refractive indexes for radiation imaging and thermal neutron detection applications will be presented.

- 1. Light guiding scintillator using large refractive index difference: The eutectic crystals have a structure in which scintillator crystal fibers of several  $\mu$ m diameter are arranged in a matrix and have excellent position-resolving performance against x-rays and charged particles [1]. However, it was extremely difficult to grow the eutectic enough large or long size, and it was impossible to grow them as a single fiber. Most recently, we proposed a novel optical-guiding crystal scintillator (OCS) [2]. It consists of halide single crystal scintillator core and glass clad. The refractive index of the halide single crystals is higher than the glass in this system. Generated scintillation light above the critical angle is totally reflected at the interface with the glass and optically waveguided like optical fibers and the scintillating fivers (fig.1-right). In OCS, the molding of the cladding and the crystal growth of the scintillator core are performed in the same process. OCS was not limited to single fiber but could also be formed into bundles for high resolution radiation imaging.
- 2. Transparent eutectic scintillator using a small refractive index difference: For the decommissioning of Fukushima Daiichi Nuclear Power Plant, fuel debris is scheduled to be removed from the primary containment vessel. Sorting is important because a large amount of fuel debris and radioactive waste are mixed and It is necessary to distinguish between gamma rays and thermal neutrons in the high-dose environment over 10Gy/h. In this field, scintillators with high sensitivity only to neutrons, fast decay (<20ns), and high neutron-gamma discrimination performance are required. Especially <sup>6</sup>Li is high thermal neutron capture cross-section elements and scintillators containing <sup>6</sup>Li have been commercialized such Ce,Eu:LiCaAlF<sub>6</sub>, Ce:Cs<sub>2</sub>LiYCl<sub>6</sub>, Tl:(Na,Li)I etc. However, there has been no scintillator that satisfies the sensitivity and fast decay required for the above application. In contrast, we have reported eutectic scintillators containing high Li concentration and scintillator phases such LiBr/CeBr<sub>3</sub>, LiBr/LaBr, LiBr/CsI etc. Scintillators must offer a high light yield and be transparent to the generated light. Sufficient transparency can be achieved by combining crystal phases with closer refractive indices. At the point view of scintillation properties, fast and high light yield scintillators such BaCl<sub>2</sub>, LaCl<sub>3</sub>, CeCl<sub>3</sub>, BaBr<sub>2</sub>, LaBr<sub>3</sub>, CeBr<sub>3</sub> with Eu<sup>2+</sup> or Ce<sup>3+</sup> doping were selected as the scintillator phase. A systematic study of combinations of each scintillators and Li-containing halides is introduced.

<sup>[1]</sup> K. Kamada, et al. Jpn. J. Appl. Phys., vol. 60, no. SB, 2021.

<sup>[2]</sup> R.Yajima, K. Kamada, et al. Ceram. Int. (2023) DOI: 10.1016/j.ceramint.2022.12.264.

#### The Effect of the Laser Beam on the width of the Cut

<u>Jana Knedlová</u><sup>1</sup>, Milena Kubišová<sup>1</sup>, Vladimír Pata<sup>1</sup>, Miroslav Marcaník<sup>1</sup>, and Barbora Bočáková<sup>2</sup>

<sup>1</sup>Tomas Bata University in Zlín, Vavrečkova 5669, Zlín, Czechia <sup>2</sup>Slovak University of Technology in Bratislava, Jána Botu 2781/25, Trnava, Slovakia

Conventional methods of dividing material due to their limitation to straight cuts have largely been replaced by non-conventional cutting methods, which include laser cutting. Laser cutting of polymer materials has become a priority for the manufacturing industry, mainly due to the constantly growing demand for these materials. The article discusses the effect of the laser beam on the width of the cut using lenses with different focal lengths, under different working conditions, on samples made of PMMA polymer material plates. For the experiment, the samples were produced using an ILS 3NM laser device, a  $CO_2$ , with a wavelength of 10.6  $\mu$ m and with maximum power 100 W, maximum feed speed 1524 mm.s<sup>-1</sup>. For the selected samples, it was studied how the dimension defined by the machining software differ from the dimension created by the machining.

#### The role of X-ray radiation in materials research

#### Marian Koman

Slovak Technical University, Faculty of Chemical and Food Technology STU in Bratislava, Radlinského 9, Bratislava, Slovakia

Before the development of X-ray diffraction crystallography, the study of crystals was based on their geometry. This involves measuring the angles of crystal faces relative to theoretical reference axes (crystallographic axes), and establishing the symmetry of the crystal in question.

Crystallographic methods now depend on analysis of the diffraction patterns of a sample targeted by a beam of some type. X-rays are most commonly used; other beams used include electrons or neutrons.

These three types of radiation interact with the specimen in different ways. X-rays interact with the spatial distribution of the valence electrons, while electrons are charged particles and therefore feel the total charge distribution of both the atomic nuclei and its electrons. Neutrons are scattered by the atomic nuclei through the strong nuclear forces, but in addition, the magnetic moment of neutrons is non-zero. They are therefore also scattered by magnetic fields. Because of these different forms of interaction, the three types of radiation are suitable for different crystallographic studies.

#### Experience with modeling values of the virtual catapult range

Janette Kotianová, Michal Turza, Zuzana Červeňanská, and Rastislav Ďuriš

Slovak University of Technology, Faculty of Materials Science and Technology in Trnava, Street J. Bottu č. 2781/25, 917 24 Trnava, Slovakia

The creation of a virtual catapult involves the synthesis of knowledge from several fields, namely physics, probability, statistics, regression analysis, and computer science. Our contribution is not focused on the description of the creation of the application from the software point of view, but it presents a method by which it is possible to generate the numerical values of the range of the virtual catapult along with their corresponding variability. When modeling these range values, it is possible to choose the classical theoretical approach, i.e., the physical approach using equations of motion, or to statistically process the measured values obtained by experimenting with a real catapult model. In our case, a statistical approach, specifically the Design of Experiments method, was chosen to estimate the values of the catapult range. The obtained appropriate regression model was used as the output of the statistical analysis of the measured data for point estimates of the range at specific settings of selected parameters of a real catapult.

In order for the results of the simulated range values to correspond to the actual range values of the catapult, it was necessary to achieve a realistic fluctuation (randomness) of the results in the simulation of the catapult ranges around the predicted range value obtained from the regression model.

This article suggests a way to ensure stochasticity when modeling such types of systems.

#### Silver phosphate glasses modified by transition metal oxides

Ladislav Koudelka, Tomáš Hostinský, and Petr Mošner

Department of General and Inorganic Chemistry, Faculty of Chemical Technology, University of Pardubice, 532 10 Pardubice, Czech Republic

Phosphate glasses of the systems Ag<sub>2</sub>O-V<sub>2</sub>O<sub>5</sub>–WO<sub>3</sub>-P<sub>2</sub>O<sub>5</sub> and Ag<sub>2</sub>O-V<sub>2</sub>O<sub>5</sub>-Nb<sub>2</sub>O<sub>5</sub>-P<sub>2</sub>O<sub>5</sub> were studied. In two compositional series of  $40Ag_2O-xV_2O_5-(1-x)WO_3-30P_2O_5$  and  $40Ag_2O-yV_2O_5-(1-x)WO_3-30P_2O_5$ (1-y)Nb<sub>2</sub>O<sub>5</sub>-30P<sub>2</sub>O<sub>5</sub>13 glasses was prepared and studied. Starting glasses without V<sub>2</sub>O<sub>5</sub>are slightly yellowish. Glasses with vanadium oxide V<sub>2</sub>O<sub>5</sub> are black due to the presence of vanadium in the form of  $V^{4+}$ . Thermal analysis showed on decreasing glass transition temperature with an increasing V<sub>2</sub>O<sub>5</sub> content in both studied series. For the glass series with WO<sub>3</sub> glass transition temperature varies within the values 392-279 °C, for Nb<sub>2</sub>O<sub>5</sub> containing glasses within the values of 572-279 °C. Glass structure was studied by Raman spectroscopy and by <sup>31</sup>P MAS NMR. The NMR spectra of 40Ag<sub>2</sub>O-xV<sub>2</sub>O<sub>5</sub>-(1-x)WO<sub>3</sub>-30P<sub>2</sub>O<sub>5</sub>glass series contain one broad resonance peaking at -4.2 - +3.1 ppm. Such position of the resonance signal corresponds to the presence of Q<sup>1</sup> diphosphate structural units. For the 40Ag<sub>2</sub>O-yV<sub>2</sub>O<sub>5</sub>-(1-y)Nb<sub>2</sub>O<sub>5</sub>-30P<sub>2</sub>O<sub>5</sub> glass series  $^{31}P$  NMR spectrum of the glass with y = 0 evidently consists of two resonances, which indicates the presence of two types of phosphate units of  $Q^1$  and  $Q^0$ . Such shape of the NMR spectrum is ascribed to the formation of Nb-O-Nb-O-Nb chains from niobate octahedra in the starting glass. These chains disappear with a decrease in the  $Nb_2O_5$  content in the glasses. Raman spectrum of the starting tungstate-phosphate glass series 40Ag<sub>2</sub>O-xV<sub>2</sub>O<sub>5</sub>-(1x)WO<sub>3</sub>-30P<sub>2</sub>O<sub>5</sub> with x = 0 reveals the dominant band of 918 cm<sup>-1</sup>, the position of which shifts slightly to lower wavenumbers with decreasing  $WO_3$  content. This band was ascribed to the vibrations of the W-O bonds in WO<sub>6</sub> octahedra. Raman spectrum of the 40Ag<sub>2</sub>O-yV<sub>2</sub>O<sub>5</sub>-(1y)Nb<sub>2</sub>O<sub>5</sub>-30P<sub>2</sub>O<sub>5</sub> glass without  $V_2O_5$  is composed of two bands The first band at 805 cm<sup>-1</sup> was ascribed to the presence of Nb-O-Nb-O-Nb chains and the second band at 896 cm<sup>-1</sup> to the vibrations of Nb-O bonds in NbO $_6$  octahedra. Final glass with  $V_2O_5$  only reveals in the Raman spectrum dominant band at 912 cm<sup>-1</sup>, assigned to the vibrations of O-V-O bonds in vanadate structural units.

#### **Energy of nuclei formation on curved active centers**

Zdeněk Kožíšek, Robert Král, and Petra Zemenová

FZU - Institute of Physics of the Czech Academy of Sciences, Cukrovarnická 10, 16200 Praha 6, Czechia

Phase transition in a parent phase (supercooled melt or supersaturated solution) occurs via the formation of nuclei of a new crystalline phase by homogeneous or heterogeneous nucleation when clusters of a new phase appear due to fluctuations within the parent phase. The probability of nucleus formation is exponentially proportional to the nucleation barrier W\*, i.e. the work of formation of critical clusters plays an important role in model approaches to the nucleation process. Exact analytical solutions for W\* are well known for homogeneous and heterogeneous nucleation on a flat surface. This work focuses on heterogeneous nucleation on foreign surfaces, which serve as active centers, where the probability of nucleus formation is higher. On curved substrates, it is much more challenging to find an analytical solution for W\*, and using a more extended model is necessary. It is well known that the critical radius of the nucleus r\* is identical for homogeneous and heterogeneous nucleation unlike the number of monomers (atoms or molecules) i\* forming the critical nucleus. Nucleation kinetics suppose a step-by-step process, when the expression for formation energy of clusters W, as a function of the number of monomers I forming the cluster, is required. It is easy to express W(r) as a function of cluster radius r, and also W(i) as a function of cluster size i for homogeneous and heterogeneous nucleation on a flat surface. Generally, W(i) is difficult to express on curved surfaces. In this work, we summarize models for analytical approaches for W on concave and convex substrates as a function of cluster size [1, 2]. The analytical expression for W(i) is too difficult to find as even analytical r(i) dependency is not easy to find. It is shown that the probability of nucleus formation on a concave substrate is higher in comparison with a convex one. Moreover, in the case of crystallization of the small droplet, i. e. small encapsulated system, the depletion of the parent phase plays an important role [3]. The formation of crystalline nuclei can be even stopped due to an insufficient number of monomers within the parent phase.

- [1] D. Xu, W. L. Johnson, *Geometric model for the critical-value problem of nucleation phe*nomena containing the size effect of nucleating agent, Phys. Rev. B 72 (2005) 052101.
- [2] S. J. Cooper, C. E. Nicholson, J. Liu, *A simple classical model for predicting onset crystallization temperatures on curved substrates and its implications for phase transitions in confined volumes*, J. Chem. Phys. 129 (2008) 124715.
- [3] Z. Kožíšek, R. Král, P. Zemenová, *Homogeneous nucleation and crystallization model of Aluminum droplet based on isothermal DSC analysis*, J. Therm. Anal. Calorim. 147 (2022) 13089.

# Simultaneous DSC-TGA-MS analyses of RE<sub>2</sub>O<sub>3</sub> compounds for growth multicomponent oxides

Robert Král, Petra Zemenová, Alexandra Falvey, Vojtěch Vaněček, Aleš Bystřický, Jan Pejchal, and Martin Nikl

Institute of Physics, Czech Academy of Sciences, Cukrovarnicka 10, Prague, Czechia

Scintillation materials are widely used as detectors of ionizing radiation (photon or particle based) in multiple fields of human activities consisting of both research & development and industrial applications. This includes fields for instance of medical imaging techniques, highenergy physics, industrial defectoscopy, geological survey and oil well logging, astronomy, homeland security and others [1]. Scintillation detectors for all these applications mostly employ inorganic materials based on single crystals of garnets, perovskites, heavy silicates, halides or other multicomponent compounds. Crystals of multicomponent compounds such as garnets and perovskites are usually prepared from their melts by traditional methods (e.g. Czochralski, Bridgman, or Kyropoul method) or by methods suitable for research screening, e.g. micropulling-down (mPD) method [2]. The mPD enables to prepare single crystals of various materials (e.g. oxides, halides, metals, etc.) with dimensions of several millimeters (3-5 mm) in diameter and several centimeters long in a very short time (in matter of hours to tens of hours) [3,4]. However, the preparation of crystals using above mentioned methods requires a compliance with precisely calculated starting composition of the input raw materials. Thus, the composition and initial purity of the raw materials are required to be determined before the crystal growth experiments.

This contribution is focused on the study of the thermal properties of rare earth oxides, e.g. lanthanum oxide ( $La_2O_3$ ), scandium oxide ( $Sc_2O_3$ ), gadolinium oxide ( $Gd_2O_3$ ), etc., which are often used as raw materials in the preparation of crystals of multicomponent oxides based on garnets and perovskites.  $La_2O_3$  was previously used, for example, in the growth of the lanthanum-aluminum perovskite LaAlO3:Ce crystal [1]. The aim of this work is to study the purity of the starting materials and to determine the optimal conditions for their treatment and storage. Such goals were achieved using simultaneous thermoanalytical methods consisting of differential scanning calorimetry (DSC), thermogravimetry (TGA), and mass spectrometry (MS). In this way one can record changes in sample(s) regarding: (i) heat flow e.g. exo- and endo-thermic effects (e.g. phase transitions, reactions, etc.), (ii) mass change (decomposition, reactions, etc.), and (iii) detection of evolved gases and their fragments. Obtained results will be presented and discussed.

- [1] J. Pejchal et al., Mater. Adv. 3 (2022) 3500–3512.
- [2] V. Vaněček et al., Advanced Photonics Research 3 (2022) 2200011.
- [3] A. Yoshikawa et al., Optical Materials 30 (2007) 6–10.

#### Statistical evaluation of hard-to-measure surfaces

Milena Kubišová<sup>1</sup>, Jana Knedlová<sup>1</sup>, Hana Vrbová<sup>1</sup>, Vladimír Pata<sup>1</sup>, and Barbora Bočáková<sup>2</sup>

<sup>1</sup>Tomas Bata University in Zlín, Faculty of Technology, Vavrečkova 5669, Zlín, Czechia <sup>2</sup>Institute of Manufacturing Technologies, Faculty of Materials Technology based in Trnava, Slovak Technical University in Bratislava

The main goal of this article will be to find ways to statistically evaluate hard-to-measure surfaces. First, the basic characteristics and rules of surface quality will be described according to the standards ČSN EN 4287, ČSN EN 4288, and ČSN EN ISO 2517-2. Subsequently, the measured values of the roughness parameter Sa (arithmetic average of the height of the measured surface) and Sz (the maximum height of the measured surface) will be compared and evaluated which is the best. [1]

These parameters will be described and measured on aluminum plates on which the test surfaces were laser engraved. To evaluate the best surface, statistical methods will be used, such as the EDA methodology (exploratory data analysis), hypothesis testing with normality and outlier tests, and last but not least, cluster or cluster analysis, which compared the similarity of the measured data. [2] This article aims to show the possibilities of surface quality assessment using 3D surface roughness parameters, which are not often used in practice.

- [1] Whitehouse, D. J. Handbook of Surface and Nanometrology; 2nd ed. Boca Raton: CRC Press; (2011) ISBN 978-1-4200-8201-2
- [2] Meloun, M.; Militký, M.; Forina, M.; Chemometrics for Analytical Chemistry; Ellis Horwood: New York (1992)ISBN 9780131263765

### New Ni(II) complexes with 2-aminomethylbenzimidazole, preparation and characterization

Vladimír Kuchtanin, Rudolf Varga, Ján Pavlik, and Ján Moncol'

Slovak University of Technology in Bratislava, Bratislava, Slovak Republic, Radlinského 9, Bratislava, Slovakia

An important class of heterocyclic compounds in many natural and synthetic compounds for the development of new drugs are benzimidazoles [1]. Use of benzimidazoles can be found in liquid crystal materials due to their special physicochemical properties based on fluorescence modulation mechanisms [2]. The benzimidazole moiety involves in a variety of biological processes. For example, N-ribosyl-dimethylbenzimidazole is part of the chemical structure of vitamin  $B_{12}$  [3]. Benzimidazole derivatives are of intensive researches due to their coordination ability besides their biological importance [4].

New Ni(II) complexes of general formula NiL $_x$ Y $_z$  have been synthesized, where L is 2-aminomethylbenzimidazole and Y are inorganic anions such as Cl $^-$ , Br $^-$ , ClO $_3$  $^-$ , ClO $_4$  $^-$ , NO $_2$  $^-$ , N $_3$  $^-$ , SCN $^-$ , SO $_4$  $^2$  $^-$  as well as organic anion CH $_3$ COO $^-$ . All newly prepared complex compounds were characterized by X-ray structural analysis and by spectral techniques such as infrared spectroscopy and UV-VIS spectroscopy. Magnetic measurements were also performed for some compounds.

- [1] Chen, R. H. et al.: Asian Journal of Chemistry (2014), 26, 926-932.
- [2] Qin, H. et al.: Org. Chem. Front. (2019), 6, 205-208.
- [3] R. Bonnett, Chem. Rev., 63 (1963), 573-605.
- [4] B. MacHura, A. Świtlicka, M. Penkala, Polyhedron, 45 (2012), 221-228.

# Development of a high-frequency rapid scan electron spin resonance spectrometer

Oleksii Laguta, Matuš Šedivý, Vinicius Santana, Andriy Marko, and Petr Neugebauer

VUT Brno, Purkynova 123, Brno, 61200, Czechia

We report on the recent development of a high-frequency rapid scan electron spin resonance (FRASCAN) spectrometer at the Brno University of Technology. The basic principle of frequency rapid scan will be explained and compared to conventional methods. The FRASCAN operates in induction mode using quasi-optics with a superheterodyne detection scheme. Fast frequency sweeps of the order of 1000 THz/s allow to access spin relaxation of the order of 1 ns [1,2], in a frequency range of 80 GHz to 1100 GHz [3], at temperatures from 1.8 K to 300 K, and at magnetic fields up to 16 T. We developed several sample holders for performing measurements on liquids, oriented single crystals, and air-sensitive samples, including the possibility of photo-excitation [3]. In addition, we developed a carousel sample holder for pressed powders that accommodates up to 6 samples, avoiding the time-consuming event of loading the probe into the cryostat and cooling down process. The carousel holder can be used for quantitative ESR. The FRASCAN is controlled by a home-written software in LabView, allowing to run experiments in an automatic mode controlled by scripts. Frequency rapid scan experiments on an oriented single crystal of LiPc will be presented along with simulation for calculation of the relaxation times. Furthermore, additional capabilities of FRASCAN are demonstrated using frequency-detected magnetic resonance spectra as a function of the orientation for a singlecrystal of copper acetate and frequency-field ESR maps for Mn<sub>12</sub> and TEMPO.

- [1] O. Laguta, M. Tuček, J. van Slageren, P. Neugebauer, J. Magn. Reson. 296 (2018) 138.
- [2] O. Laguta, A. Sojka, A. Marko and P. Neugebauer, Appl. Phys. Lett. 120 (2022) 120502.
- [3] A. Sojka, M. Šedivý, A. Solodovnik, A. Lagin, T. Láznička, V. Santana, A. Marko, O. Laguta and P. Neugebauer, IEEE Trans. Instrum. Meas. 71 (2022) 1.

# Activation function as an inspiration for metamaterial design and gyroid as inspiration for activation function design. Part 2: next contexts

Roman Budjač<sup>1,2</sup>, <u>Iveta Markechová</u><sup>1</sup>, and Hana Stúpalová<sup>1</sup>

<sup>1</sup>Slovak University of Technology, Faculty of Materials Science and Technology, Jána Bottu 2781/25, 917 24 Trnava, Slovakia <sup>2</sup>University of Žilina, Research centre, Univerzitná 8215/1, 010 26 Žilina, Slovakia

Metamaterials represent a relatively new field of research. Our previous approach to their design was to create a translational surface from some type of mathematical curve. Elliptical curve and sigmoid have dominated. Mostly by linear transformations of the translational surface as such, and also by replicating it or by transformed replication we created different structures of metamaterials. In the current work, we were partly inspired by the work of researchers from MIT and their original approach in creating the so-called procedural metamaterials.

Continuation of our investigation of planar cutting curves on the gyroid showed surprising possible connections of their shape, under specific input conditions, with phonon modes for periodic structures with glide symmetry. Here we finger them out.

Research work with the sigmoid and gyroid bring us several inspirations, for example for the field of applications in biomedicine, in student education and in educational work for lay people. Please, familiarize yourself with them via this output of our research work.

#### Degradation of rubber compounds under natural conditions

<u>Lenka Markovičová</u>, Viera Zatkalíková, Milan Uhríčik, and Silvia Hudecová *University of Žilina*, *Univerzitná 8215/1*, *Žilina*, *Slovakia* 

Rubber compounds are complex, chemically active and viscoelastic materials. The resulting rubber compounds are made up of a mixture of elastomers and fillers such as carbon black, silica, kaolin, calcium carbonate and others. A very important element of which rubber compounds are composed is sulphur. Its important function is to ensure the cross-linking process during vulcanisation. Lubricants, plasticizers and various organic substances that are used to modify the properties are also essential components of rubber compounds.

Rubber recycling is the process of repurposing irreparably damaged or worn rubber products (natural or synthetic) for new uses in order to prevent rubber waste from ending up in landfills. The process or recycling and reusing rubber requires less energy) less stress on natural rubber, saving landfill space and reducing pollution) than making new rubber. Most of the rubber for the rubber recycling industry comes from waste tires. The rubber recycling industry converts waste rubber products into usable material that can be used to make new rubber products. Waste rubber can also be converted into fuel.

In the typical rubber recycling process, rubber is collected, shredded, sorted, and finally devulcanized to transform waste rubber into raw material. Devulcanization of rubber waste is a process that reverses the vulcanization of rubber, recycling it so that it can be vulcanized again. This process converts waste rubber into a new "virgin" raw material. The devulcanized rubber can be mixed with virgin rubber or with other kinds of matrices to give new compounds without generating a significant decrease in mechanical and physical properties. In addition, there are other options for processing waste rubber, such as freezing or pyrolysis of rubber waste.

This article deals with the possibilities of recycling rubber waste in natural conditions. The factors that influence the rate and extent of degradation of rubber compounds under natural conditions are temperature, humidity, pH, UV radiation, microorganisms. Test samples of rubber compounds were exposed to dry and moist soil for 1, 2 and 3 months. The samples were evaluated for the change in selected mechanical properties, weight change and surface degradation of the samples were observed by light microscopy. Based on the result, there is a slow degradation of the rubber compound under natural conditions in wet soil, which manifested by a change in the pH of the environment, a decrease in mechanical properties. Negative changes in the surface topography were observed on the light microscope. These changes were more pronounced with increasing exposure time of the samples.

#### Possible methods of removing PCBs from environment

Jaroslava Maroszová

Faculty of Chemical and Food technology, STU in Bratislava, Slovakia, Radlinského 9, Bratislava, Slovakia

Polychlorinated biphenyls (PCBs) are physically and chemically very stable substances with serious negative effect on health. On the human organism, as well as on the surrounding environment. In addition to acute symptoms in the form of dermatoses or nausea, their toxicity is mainly chronic in the form of hepato-, nephro-, neuro-, immuno- and other toxicities, including hormonal disruption and disorders of the excretory system. Due to their optimal physicochemical properties they were massively produced all over the world. An important producer of these substances was the plant in the east of Slovakia - Chemko Strážske. Following the identification of serious toxic effects on health and the environment, the production of PCBs has been phased out worldwide (in Czechoslovakia as one of the last countries in 1984). However, as a result of the ban on production and distribution, a large amount of these substances remained in the premises of the former plant and its surroundings, together with the by-products of their production, as a significant toxicological risk. It's hard to imagine that this issue has been ignored for more than 30 years. In January 2020, a state of emergency was declared in connection with the situation in Strážské. Subsequently, a series of measures was launched to eliminate this environmental burden. The Faculty of Chemical and Food Technology (FChPT) of Slovak University of Technology (STU) is significantly involved in solving the situation in Strážské as a partner of the Ministry of the Interior of the Slovak Republic and the Ministry of the Environment of the Slovak Republic.

# Possibilities of analyzing the mechanical properties of welded and soldered joints

Maroš Martinkovič and Pavel Kovačócy

Faculty of Material Science and Technology SUT, Trnava, Slovak Republic, J. Bottu 25, Trnava, Slovakia

The quality criterion of a welded and soldered or brazed joint is its integrity, shape and mechanical properties [1]. Quantitative expression of mechanical properties are mechanical characteristics, determined by testing. Hardness, strength and toughness are the most frequently tested for welded joints. During the microhardness test [STN EN ISO 9015-2], the hardness can be measured in all parts of the weld joint, which consists of the base material, the heat-affected zone and the weld metal. During the toughness test [STN EN ISO 9016], the toughness can also be measured in all parts of the weld joint by a suitable sample selection and a suitable notch situation. For test strength [STN EN ISO 4136] it is more complicated. The sample breaks at the point of least strength or at the point of the defect. If there is a violation in the basic materials, the joint is evaluated as satisfactory, but we do not get an overview of the strength of the individual parts of the welded joint and also of the soldered or brazed joint. Often in this case, notches are applied to different parts of the weld joint, but the failure often proceeds from the notch to other parts of the joint that have lover strength. Thus, it is not possible to measure the strength in a predetermined part of the weld joint and also the strength of the soldered or brazed joint. An option to measure this property is to measure the shear strength in the active predetermined part of the weld joint. It is thus possible to measure shear strength in butt weld joints in basic materials, in various zones of the heat-affected zone, in weld metal and also in lap welded joints and soldered joints [2]. From the force-displacement dependence, it is possible to determine the toughness for a given area. The possibilities of analyzing the mechanical properties in the mentioned way were verified on butt and lap joints and on the basis of this, technological parameters were optimized.

- [1] Cheng, Z., Huang, J., Ye, Z., Chen, Y., Yang, J., Chen, S.: Microstructures and mechanical properties of copper-stainless steel butt welded joints by MIG-TIG double-sided arc welding. J. Mater. Process. Tech 265, 87–98 (2019).
- [2] Martinkovič, M., Kovačócy, P.: Equipment for measuring the mechanical properties of a welded joint in a tensile testing machine. Utility Model Number (2020). https://wbr.indprop.gov.sk/WebRegistre/UzitkovyVzor/Detail/238-2020

# Single crystal gowth of Ru-Mo-W-Re alloy wire by the dewetting micro-pulling-down method

<u>Rikito Murakami</u><sup>1,2</sup>, Shiika Itoi<sup>2</sup>, Kotaro Yonemura<sup>1,3</sup>, Kei Kamada<sup>2,4</sup>, and Akira Yoshikawa<sup>1,2,4</sup>

<sup>1</sup>Institute for Materials Research, Tohoku University, 2-1-1, Katahira, Sendai, Miyagi, Japan <sup>2</sup>C&A Corporation, Sendai, 980-0811, Japan

<sup>3</sup>Graduate School of Engineering, Tohoku University, Sendai, 980- 8579, Japan <sup>4</sup>New Industry Creation Hatchery Center, Tohoku University, Sendai, 980-8579, Japan

**Backgrounds:** Recently we have developed a novel Ru-Mo-W alloy (Ruscaloy) wire for resistance heating element that improves energy efficiency in the vacuum deposition method such as for the organic electroluminescent thin film deposition [1]. Ru-based alloys are known its brittleness due to the intergranular fracture, however, the dewetting micro-pulling-down (  $\mu$ -PD) method enables to make single-crystal wire from the melt [2]. Although Ruscaloy has a melting point of 2345 K, higher melting point and more reasonable value expand the usage (e.g., deposition of columnar scintillators), thus we tried to substitute Ru with Re whose melting point is 3459 K and its cost is 10 times lower. Additionally, reactivity with halides were compared with the conventional polycrystalline Ta wire.

**Experiments and results:** Raw materials with the purity of >99.9 % were firstly melted into button ingots using arc-melting furnace, and  $Ru_{60-x}Mo_{15}W_{25}Re_x$  (x = 1, 10, 15 at. %) alloy wires were grown by the dewetting  $\mu$ -PD method using yttria doped zirconia crucible. The diameters of the grown crystals were 0.8 mm and the length were 14.2, 2.4, and 1.7 m, respectively. The grown crystals were cut and annealed at 2273 K for 3h in high purity argon atmosphere. Compositional analysis and crystal orientation analysis were performed by wavelength-dispersive X-ray fluorescence spectroscopy (WDX) and electron beam backscatter diffraction (EBSD). Electrical resistivity was measured at room temperature by the four-terminal method, and room-temperature tensile tests were performed.

The grown  $Ru_{0.59}Mo_{0.15}W_{0.25}Re_{0.01}$  wire was single crystal oriented in the [2-1-10] direction and showed a maximum tensile strength of 658 MPa and fracture elongation of 89%, showing a suitable level of mechanical properties for heating elements. For compositions with high Re concentration, optimal temperature control was more difficult because the melting points were closer to the zirconia crucible. However, it was demonstrated for the first time that producing wires of a high Re content alloy is possible. The thermodynamic calculations on the solidus temperature and the reactivity with halides will also be reported in the presentation.

- [1] R. Murakami, A. Yoshikawa et al., Int. J. Refract. Met. Hard Mater. 114 (2023) 106235.
- [2] R. Murakami, A. Yoshikawa et al., ACS Omega 6 (2021) 8131–8141.

# Effect of structural modification of rotor with a flexible shaft on its modal properties

Milan Nad', Peter Bucha, and Ladislav Rolník

Slovak University of Technology, Faculty of Materials Science and Technology, Ul. J. Bottu 25, 917 24 Trnava, Slovakia

The rotor structures are basic systems that realize the transfer of rotary motion in technical devices and systems. The structure and the mass distribution of the rotor have a fundamental influence on the dynamic properties of the rotor. Improper geometry of the rotor structure cause the emergence of various unacceptable phenomena. These phenomena are usually caused by the rotational inertia effects of the rotor, as well as the stiffness of bearings [1] and they affect the rotor resonant states. Unfavorable phenomena arising during rotor operation [2] can be eliminated or minimize already by appropriate modification of the rotor structure. The rotor modifications can be performed mainly by modifying the rotor's rotational mass, increasing the rotor's stiffness, or changing the stiffness of bearings. As a result of these modifications, it is possible to achieve such values of natural frequencies, i.e. critical rotor speeds that are outside the operating speed range. It is obvious that in the case of a change in the operating regime, the undesirable conditions may occur, i.e. the rotor operates at operating speeds that were not taken into account in the design process of the rotor. For this operating condition, the rotor has unsuitable dynamic parameters, and therefore it is necessary to eliminate undesirable dynamic effects and their transmission to the production equipment, or to the work environment. One of the possibilities of eliminating these undesirable conditions is the design of such a rotor structure [3] that will allow the redistribution of mass and stiffness properties of the rotor during operation. The aim of the study is the analysis of the influence of mass and stiffness parameters of the rotor on the dynamics of selected types and structures of rotors. The solution and analyzes of the modal properties of the rotors are performed for two rotor structures - a rotor with a rigid disc between the bearings and a rotor with an overhanging disc. The following modifications of the structural elements of the rotor and their influence on the modal properties of the considered types of rotors are investigated - geometry and material properties of the binding layers in which the bearings are inserted; - the influence of the reinforcing core position and length inserted into the rotor shaft.

- [1] Adams, M. L. Jr., Rotating Machinery Vibration-From Analysis to Troubleshooting, Marcel Dekker, Inc. New York-Basel. 386 p., ISBN 0-8247-0258-1. 2001.
- [2] Lalanne, M., Ferraris, G. Rotordynamics Prediction in Engineering, Lyon, France: John Wiley & Sons, 1991, 252 p., ISBN 0-8247-2399-6.
- [3] Nad, M. Modification of Modal Characteristics of Vibrating of Structural Elements. Scientific Monographs, Hochschule Anhalt, Koethen, 2010, ISBN 978-3-86011-029-4.

#### Assessment of cutting tool wear using a numerical FEM simulation model

Martin Necpal

MTF STU, Ul. Jána Bottu, Trnava, Slovakia

The advancement of computational modeling techniques, such as FEM, has enabled to simulate complex machining processes with improved accuracy. Wear prediction is a crucial aspect in understanding and optimizing machining processes, as it directly impacts tool life, surface quality, and overall machining efficiency. This work focuses on the FEM simulation, specially utilizing the DEFORM software, in conjunction with the Usui wear model, for wear prediction in machining operations. The Usui wear model, a well-established and widely used wear prediction approach, accounts for multiple wear mechanisms including adhesion, abrasion, and diffusion. By incorporating the Usui wear model into the FEM simulation framework within DEFORM software, it is possible to understanding wear phenomena in machining processes. The integration of Usui wear model algorithms into DEFORM, the simulation enables the accurate prediction of wear rates, distribution patterns, and progression of tool deterioration. This predictive capability facilitates the identification of critical wear zones and guides proactive measures to enhance tool life, reduce production costs, and optimize machining productivity. This work presents a research focused on wear prediction in cutting processes, utilizing finite element simulation with DEFORM software and incorporating the Usui wear model. Through the comprehensive analysis of wear phenomena, this research aims to optimize cutting parameters, enhance tool life, and contribute to the advancement of machining and manufacturing technologies.

### NV spin qubit systems: a platform from sensing to quantum computation

Milos Nesladek

Hasselt University, Martelarenlaan 42, Hasselt, Belgium

The abstract has not been sent.

# Crystal Growth and Optical Properties of Ce-doped (Y, Tb)<sub>3</sub>Al<sub>2</sub>Ga<sub>3</sub>O<sub>12</sub> and (Gd, Tb)<sub>3</sub>Al<sub>2</sub>Ga<sub>3</sub>O<sub>12</sub> Scintillators

Kazuya Omuro<sup>1,2</sup>, Masao Yoshino<sup>2,3</sup>, Kei Kamada<sup>2,3,4</sup>, Kyoung Jin Kim<sup>2</sup>, Takahiko Horiai<sup>2,3</sup>, Rikito Murakami<sup>2</sup>, Akihiro Yamaji<sup>2,3</sup>, Takashi Hanada<sup>2</sup>, Yuui Yokota<sup>2</sup>, Shunsuke Kurosawa<sup>2,3,5</sup>, Yuji Ohashi<sup>2,3</sup>, Hiroki Sato<sup>2,3</sup>, and Akira Yoshikawa<sup>2,3,4</sup>

<sup>1</sup>Graduate School of Engineering, Tohoku University, Japan
<sup>2</sup>Institute for Materials Research, Tohoku University, Japan
<sup>3</sup>New Industry Creation Hatchery Center, Tohoku University, Japan
<sup>4</sup>C&A Corporation, Japan
<sup>5</sup>Institute of Laser Engineering, Osaka University, Japan

**Introduction** Scintillators are widely used in X-ray imaging, which are applied for medical diagnostics and airport security controls. To obtain images with excellent contrast in short exposure times, scintillators are required to have the high light output. Therefore, Tb-doped scintillators are noble candidate for X-ray imaging [1]. Recently, Ce and Tb co-doped scintillators such as Ce-doped (Gd, Tb)<sub>3</sub>(Al, Ga)<sub>5</sub>O<sub>12</sub> (GAGG:Ce, Tb) have been explored due to efficient energy transfer between  $Ce^{3+}$  and  $Tb^{3+}$ , which enable to improve the luminescence and scintillation properties [2]. However, the absorption spectra of GAGG show the peaks associated with  $Gd^{3+}$  4f-4f transitions which overlap the absorption bands associated with  $Tb^{3+}$  4f-5d transitions [3]. As a consequence, the presence of Gd in the host material introduces complexity to the behavior of energy transfer between  $Ce^{3+}$  and  $Tb^{3+}$  and presents challenges in its elucidation. To investigate the specific influence of Gd within the host material on the energy transfer between  $Ce^{3+}$  and  $Tb^{3+}$ , we conducted a comprehensive study of the optical and scintillation properties of Ce-doped (Y, Tb)<sub>3</sub> $Al_2Ga_3O_{12}$  (YAGG:Ce, Tb). Through a comparative analysis of these properties with those of GAGG:Ce, Tb, our aim was to attain a more distinct understanding of the role of Gd as a host material.

**Materials and Methods** A stoichiometric mixture of 4N CeO<sub>2</sub>,  $Tb_4O_7$ ,  $Gd_2O_3$ ,  $Y_2O_3$ ,  $Ga_2O_3$  and  $Al_2O_3$  powders was used as starting material. Ce and Tb co-doped YAGG and GAGG crystals were grown by the micro-pulling-down method. Crystals were grown from an Ir crucible under the  $Ar+2\%O_2$  atmosphere and GAGG crystals were used as seed.

**Results** We were succeeded in growing transparent YAGG and GAGG crystals. Under excitation into  $Ce^{3+}$  4f-5d band at 430 nm, the typical emission spectra associated with the  $Ce^{3+}$  and  $Tb^{3+}$  were simultaneously observed in both crystals. However,  $Tb^{3+}$  emission of YAGG crystal had higher intensity than that of GAGG crystal. The results of photoluminescence decay times and scintillation properties measurement will be presented in the conference.

- [1] K. Kamada, A. Yoshikawa, et al., IEEE Trans. Nucl. Sci. 65 (2018) 2036-2040.
- [2] T. Wu, et al., Materials 15 (2022) 2044.
- [3] A. Markovskyi, et al., J. Alloys Compd., 849 (2020) 155808.

#### Influence of selected parameters of drag finishing on tool microgeometry

Boris Pätoprstý, Marek Vozár, Tomáš Vopát, Ivan Buranský, and František Jurina

Faculty of Materials Science and Technology in Trnava, Slovak University of Technology in Bratislava, Ulica Jána Bottu č. 2781/25, Trnava 917 24, Slovakia

The aim of the experiment described in the paper was to determine how selected parameters of drag finishing such as process time, immersion depth and rotation frequency affect microgeometry of cutting edge. Four flute cemented carbide mills with diameter of 10 mm were used in this experiment. These mills were drag finished on prototype drag finishing machine developed on Faculty of Materials Science and Technology, Slovak University of Technology. Alicona Infinte Focus SL measuring machine was used to measure microgeometry of these mills. The main parameter of microgeometry of cutting edge was the size of the radius of cutting edge. In the article we compared which parameter has the biggest influence on size of cutting edge radius and also there was statistical evaluation carried out. The most significant parameter of drag finishing was determined to be the immersion depth.

# Morphology of selected multicomponent garnet laser crystals grown by micro-pulling-down method

Jan Pejchal<sup>1</sup>, Jan Havlíček<sup>2</sup>, Jan Šulc<sup>3</sup>, Karel Nejezchleb<sup>2</sup>, Helena Jelínková<sup>3</sup>, and Martin Nikl<sup>1</sup>

<sup>1</sup>Institute of Physics, Czech Academy of Sciences, Cukrovarnická 10, Prague, Czech Republic

<sup>2</sup>Crytur Ltd., Na Lukách 2283, Turnov, 51101, Czech Republic

<sup>3</sup>Czech Technical University in Prague, Faculty of Nuclear Sciences and Physical

Engineering, Břehová 7, Prague, 11519, Czech Republic

Tm- and Ho-doped multicomponent garnet laser crystals are intended for laser generation around 2  $\mu$ m [1]. Due to the disordered structure of these multicomponent crystals, the absorption and emission lines of the doping ions are significantly spectrally broadened, which is advantageous both for efficient diode pumping and for wide laser tunability or for the generation of very short pulses in mid-infrared spectral region. Possible applications of such lasers include medical applications, high-resolution spectroscopy, and remote sensing. Moreover, the Tm<sup>3+</sup> ions can be used as effective sensitizers for the Ho<sup>3+</sup> ions responsible for laser action around 2.05-2.15  $\mu$ m [1].

We have prepared the Tm-doped, Ho-doped and Tm,Ho-codoped multicomponent garnet single crystals with different dopant concentrations by the micro-pulling-down method [2, 3] using two types of crucibles. One was a classical crucible with 3 mm diameter circular shaped die with one 0.5 mm capillary. The crystals could be grown well without cracks or any visible inclusions. However, observations with a microscope under polarized light showed significant inhomogeneities, deteriorating the optical properties and laser action of the samples. Therefore, we have changed the crucible design in a way that the 3 mm diameter die included a 2 mm diameter orifice enabling better contact of the melt and the emerging crystalline phase. Such a design led to the crystal homogeneity improvement and the resulting positive influence on the optical properties. We have also tested a conical crucible without a die with a simple 2 mm circular orifice in the conical bottom, where even better contact with the melt and the growing crystal could be achieved and the homogeneity was even further increased due to smaller crystal diameter and reduced thermal stress caused by steep temperature gradients usually present in the micro-pulling down growth process.

The details and peculiarities of the crystal growth of the Tm, Ho-doped/codoped multicomponent garnet crystals, their morphology and homogeneity will be discussed in relation to the crucible design. The optical and luminescence properties will be shown and the capability of the laser action of selected crystals in the region of interest will be demonstrated.

- [1] B. M. Walsh, Laser Phys. 19 (2009) 855.
- [2] A. Yoshikawa, M. Nikl, G. Boulon and T. Fukuda, Optical Materials 30 (2007) 6.
- [3] A. Yoshikawa, V. Chani, MRS Bulletin 34 (2009) 266.

# Metal Chalcogenides for Thermoelectricity, Solar Cells and Optoelectronic Devices

#### Michal Piasecki

Jan Dlugosz University in Czestochowa, Armii Krajowej 13/15, Czestochowa, Poland Uzhhorod National University, 46 Pidhirna , Uzhhorod, Ukraine

Searching the new materials with desired properties and optimization of their synthesis methods is one of very important directions of physics development. It allows to get research objects to verify new hypotheses or confirm predictions of advanced theoretical concepts (e.g. topological materials  $Pb_{1-x}Sn_xSe$ ). From the other hand, concerning the engineering materials, it is important to obtain optimal, desired properties (efficiency, durability, non-toxicity, manufacturing costs) for particular applications.

In my talk I focus on establishing the fundamental relationship between chemical composition, crystallographic structure and physical properties (thermoelectricity, NLO, solar cells, dosimetry, Mid-Red luminescence) and then I would like to explain laser stimulated effects such as change in absorption, piezo-optical properties, intensity of the second and third harmonics of light or the phenomenon of luminescence. This allowed to determine which chemical bonds or kind of defects and their concentration in the crystallographic structure have a crucial influence on the observed relationships. This knowledge gives the possibility of introducing effective modifications of particular compounds by creating new crystals, solid solutions, doping, low dimensionality and improving the growth technology in order to achieve the desired properties.

An important element of the lecture will be the issue of chalcogenide single crystals for which we additionally conducted comprehensive studies of crystallographic and electronic structures using the XRD method, XPS and XES photoelectron spectroscopy. Because the XPS and XES studies allow to determine not only the total density of electron states in the valence band, but also the partial contribution to total density of states from individual atoms, after DFT calculations it is possible to check the agreement between the calculated and experimental data. In addition, I put a special emphasis on the experimental determination of the band gap, activation energy and their dependence on temperature, structure of defect etc., which is also an additional important procedure to verify the prediction of computational methods. I will discuss and compare between the results of calculations with relevant optical measurements performed in a wide spectral range, NLO effects, photoconductivity and piezo-optics. In convincing manner, I demonstrate that the electron properties and material constants of chalcogenide crystals can be changed in a wide range by means of laser irradiation (the photo-induction process), tune composition, changes of structure and nano-effects.

#### Bioactivity of carboxylatocopper(II) complexes

#### Miroslava Puchoňová and Flóra Jozefíková

Faculty of Chemical and Food technology, STU in Bratislava, Radlinského 9, Bratislava, Slovakia

Copper complexes containing N-donor ligands are traditionally studied from different points of view, e.g. for their anti-inflammatory and anticancer properties. Of particular interest is the potential property of copper(II) complexes mimicking enzymes like the superoxide dismutase (SOD) [1-3].

In the present work we focused on studying the structural, spectral, and potential biological properties of Cu(II) complexes with various derivatives of benzoic acid and with neutral N-donor ligand 4-pyridylmethanol. Their summary formula is  $[Cu(XCOO)_2(4-PM)_2(H_2O)_x]$ , where  $XCOO^-$  presents derivatives of benzoic or fenamic acid; 4-PM =4-pyridylmethanol and x = 0 or 1. The structures of the newly prepared complexes were determined by single-crystal X-ray analysis. The complexes were characterized by spectroscopic methods (IR, UV-vis and EPR spectroscopy) and their redox properties were determined by cyclic voltammetry. The interaction of Cu(II) complexes with calf-thymus DNA was monitored by diverse techniques (UV-vis spectroscopy, viscosity measurements) suggesting intercalation as the most possible mode of binding. Furthermore, their SOD and catechol oxidase mimetic activity were studied.

- [1] M. Devereux, D. O'Shea, M. O'Connor, H. Grehan, G. Connor, M. McCann, G. Rosair, F. Lyng, A. Kellett, M. Walsh, D. Egan, B. Thati, Polyhedron 26 (2007) 4073.
- [2] M. Puchoňová, J. Švorec, Ľ. Švorc, J. Pavlik, M. Mazúr, Ľ. Dlháň, Z. Růžičková, J. Moncoľ, D. Valigura, Inorg. Chim. Acta 455 (2017) 298.
- [3] F. Jozefíková, S. Perontsis, K. Koňáriková, L. Švorc, M. Mazúr, G. Psomas, J. Moncol. J. Inorg. Biochem. 228 (2022) 111696.

# The comparison of photoluminescence decay in YAG:Er, ZnO and $SiO_2$ crystals

Zdeněk Remeš<sup>1</sup>, Maksym Buryi<sup>1</sup>, Štěpán Remeš<sup>1,3</sup>, Radim Novák<sup>1,3</sup>, Jan Pejchal<sup>1</sup>, Oleg Babčenko<sup>1</sup>, and Júlia Mičová<sup>2</sup>

<sup>1</sup>Institute of Physics CAS, Na Slovance 1999/2, Prague 8, Czechia
<sup>2</sup>Institute of Chemistry SAS, Dubravska cesta 9, 84538 Bratislava, Slovakia
<sup>3</sup>Gymnázium Christiana Dopplera, Zborovská 621/45, 150 00 Praha 5 - Malá Strana,
Czechia

We report on the intensity and time resolved photoluminescence (PL) measurements in the visible spectral range at wavelengths 350-800 nm using the phase delay method under sine wave UV excitation. Yttrium aluminium garnet (Y<sub>3</sub>Al<sub>5</sub>O<sub>12</sub>, YAG), zinc oxide (ZnO) and silicon oxide (SiO<sub>2</sub>) are crystalline materials, known for their excellent optical properties and mechanical, chemical and temperature stability. The YAG:Er crystals were grown by the micro-pullingdown method at the Institute of Physics in Prague [1], ZnO crystals by hydrothermal growth at the Institute of Chemistry in Bratislava [2] and the SiO<sub>2</sub> micro powder was purchased from Sigma-Aldrich and expoosed to inductively coupled plasma (ICP) at the Institute of Physics to create surface-related defects. Their PL spectra were measured at a room temperature using the UV LED sine wave modulated by 50 MHz Keithley 3390 generator, dispersive monochromator, 10 MHz red-enhanced photomultiplier, 1 MHz current amplifier 10<sup>5</sup> V/A, 200 MHz oscilloscope, and a 100 kHz lock-in amplifier. The sensitivity of the oscilloscope is about 3 orders of magnitude lower than the sensitivity of the lock-in amplifier. Our setup allows to measure the mean PL decay with a time resolution of about 10 ns at 100 kHz. While YAG:Er shows well resolved PL peaks with mean decay time of several  $\mu$ s related to the Stark splitting of Er<sup>3+</sup> (4f<sup>11</sup>) states, the defect-related PL spectra of ZnO and SiO<sub>2</sub> show broad defect-related bands with significantly faster mean decay times (in the order of tens or hundreds ns in ZnO, depending on doping, and below 10 ns in SiO<sub>2</sub>).

- [1] M. Buryi, et al., The role of Er3+ content in the luminescence properties of Y3Al5O12 single crystal: Incorporation into the lattice and defect states creation, Crystals 13 (2023) 562(1-14).
- [2] M. Buryi, at al., Peculiarities of erbium incorporation into ZnO microrods at high doping level leading to up conversion and the morphology change. Influence on excitonic as well as shallow donor states, Appl. Surf. Sci. 611 (2023) 155651(1-14).

#### How many electronic study resources is too much?

Kateřina Rubešová and Vít Jakeš

University of Chemistry and Technology, Technická 5, Praha 6, Czechia

With the development of information technology, we were ecstatic about the possibilities opened up for educators in the field of electronic teaching tools. More than 10 years ago, at the University of Chemistry and Technology in Prague (UCT), we started creating both passive and interactive electronic study materials, and we were excited to be able to engage today's generation of students with something other than a printed book. As a part of European or national development projects, as well as within the Pedagogical Internal Grant Agency of UCT, a large number of tools were created, some of which still bear the marks of our "learning how to do it".

Then, Covid19 together with distance teaching occurred. Immediately, we were forced to adopt electronic teaching tools and, at the same time, to create another volume of study materials. After the end of this period, the development of electronic materials continues, but educators and students are beginning to get overwhelmed. In addition, many materials created during distance learning would deserve to be reworked into a "standard" form and level.

This presentation summarizes the electronic tools and study resources used in the teaching of General and Inorganic Chemistry, Chemical Calculations and basic inorganic laboratories in the 1st study year at UCT. The benefits or negatives of those compared to face-to-face teaching and "paper" study materials will be discussed. The presentation will also show the possibilities of electronic testing and examination, as well as the possibilities of databases and the generator of paper tests within the Moodle system.

# Effect of welding mode on selected properties of additively manufactured AA5087 aluminium alloy parts

<u>Martin Sahul</u><sup>1,2</sup>, Miroslav Sahul<sup>1</sup>, Ladislav Kolařík<sup>1</sup>, Tomáš Němec<sup>1</sup>, Marie Kolaříková<sup>1</sup>, and Barbora Bočáková<sup>3</sup>

 <sup>1</sup>Department of Manufacturing Technology, Faculty of Mechanical Engineering, Czech Technical University in Prague, Technická 4, 160 00 Prague 6, Czech Republic
 <sup>2</sup>Institute of Materials Science, Faculty of Materials Science and Technology in Trnava, Slovak University of Technology in Bratislava, J. Bottu 25, 917 24 Trnava, Slovakia
 <sup>3</sup>Institute of Production Technologies, Faculty of Materials Science and Technology in Trnava, Slovak University of Technology in Bratislava, J. Bottu 25, 917 24 Trnava, Slovakia

Wire and arc additive manufacturing (WAAM) is a popular direct energy deposition (DED) method for production of large-scale metallic components [1-3]. The main advantages of the technique are high deposition rate and low cost [4]. Furthermore, utilization of the WAAM is very popular in aerospace industry [5,6]. The AA5087 aluminium alloy with 4.5 wt.% of magnesium has been investigated because of its very good mechanical properties [7]. The present research deals with the study of thermal cycles and fields developed in the alloy during additive manufacturing with three different Cold metal transfer (CMT) modes, namely conventional (CMT), pulse (CMT-P) and cycle-step (CMT-CS). The welding system was equipped with a Fronius TransPulse Synergic 3200 CMT power source, a Fanuc Arc Mate 1000iC 6-axes robot with a R 30iA control unit, welding torch and 1-axis positioner. The AA5087 aluminium alloy welding wire with diameter of 1.2 mm was deposited onto AA5083 aluminium alloy plate with dimensions of 70 mm x 200 mm x 3 mm during the experiment. The thermal cycles were documented using Ahlborn Almemo 5690-2 measuring station equipped with K type thermocouples. The thermal fields were monitored with FLIR E95 thermography camera. The results showed the evident influence of arc mode on the temperatures developed in manufactured aluminium alloy parts during the process of WAAM.

- [1] F. Wang, J. Wei, G. Wu, M. Qie, and Ch. He, Mater. Lett. 342 (2023) 134312.
- [2] Ch. Chen, G. Sun, W. Du, J. Liu, and J. Zhang, Int. J. Mech. Sci. 238 (2023) 107831.
- [3] J. Wang, K. Zhu, W. Zhang, X. Zhu, and X. Lu, J. Mater. Res. Technol. 22 (2023) 982-996.
- [4] A. K. Sinha, S. Pramanik, and K. P Yagati, Measurement 200 (2022) 111672.
- [5] S. Zhou, K. Wu, G. Yang, B. Wu, L. Qin, X. Guo, and X. Wang, Mater. Sci. Eng. 876 (2023) 145154.
- [6] M. M. Tawfik, M. M. Nemat-Alla, and M. M., Dewidar, J. Mater. Res. Technol. 13 (2021) 754-768.
- [7] Z. Liao, B. Yang, M. Neil James, J. Li, S. Xiao, and S. Wu, Int. J. Fatigue 165 (2022) 107189.

# Influence of generator parameters on cutting width during WEDM process

#### Vladimír Šimna

Slovak University of Technology in Bratislava, Faculty of Materials Science and Technology in Trnava, , Jana Bottu 25, Trnava, Slovakia

The aim of the paper is to analyse the influence of selected parameters on the cutting width in Wire Electric Discharge Machining. Parameters with variable values were pulse width, servo reference mean voltage, time between two pulses, frequency and wire feed speed. The response was measured on a Zoller Genius 3s and Alicona InfiniteFocusSL. The most influential variable input parameter is the mean reference voltage. With a big lead with a percentage share of up to 82.4%, it is almost 15 times more influential as the second most influential factor (pulse width). At its first level, the width of the cut reaches a record low value. On the other hand, at the third level, it is again the highest value of the width of the cut.

### Tribological performance of nanolaminate coatings based on tungsten and niobium nitrides

<u>Kateryna Smyrnova</u><sup>1</sup>, Martin Sahul<sup>1</sup>, Marián Haršáni<sup>2</sup>, Alexander Pogrebnjak<sup>1,3</sup>, Lubomír Čaplovič<sup>1</sup>, Vyacheslav Beresnev<sup>4</sup>, Mária Čaplovičová<sup>5</sup>, and Martin Kusy<sup>1</sup>

<sup>1</sup>Faculty of Materials Science and Technology, Slovak University of Technology in Bratislava, Jána Bottu, 25, 917 24 Trnava, Slovakia

<sup>2</sup>Research and Development Department, Staton, s.r.o., Sadová 1148, 038 53 Turany, Slovakia;

<sup>3</sup>Department of Nanoelectronics and Surface Modification, Sumy State University, Rymskogo-Korsakova 2, 40007 Sumy, Ukraine

<sup>4</sup>Department of Materials for Reactor Building and Physical Technologies, V.N. Karazin Kharkiv National University, Svobody Sq. 4, 61022 Kharkiv, Ukraine

<sup>5</sup>Centre for Nanodiagnostics of Materials, Slovak University of Technology in Bratislava, Vazovova 5, 812 43 Bratislava, Slovakia

The automotive and aerospace industries widely utilize cutting tools in their manufacturing processes such as knurling, milling, chamfering, turning, drilling, and honing. However, optimizing production costs and using lubricants is an urgent matter. It can be achieved by using a protective hard coating on the surface of the cutting tool. Multilayer transition metal nitrides are extensively utilized for such purposes due to their high functional properties. The present study is focused on WN/NbN nanolayer coatings deposited by CA-PVD on stainless steel substrates. The effect of the substrate bias voltage (-50 V, -100 V, and -200 V.) on the microstructure and tribomechanical properties of multilayers was comprehensively studied.

The N content was approximately 50 at.% in all coatings. However, the niobium concentration slightly increased from 27 to 29 at.%, and the tungsten content reduced from 24 to 21 at.% when bias voltage changed from -200 to -50 V. The bilayer period (  $\Lambda$ ) of the nanolayer deposited at -50 V was 13 nm, and U<sub>s</sub> of -200 V reduced  $\Lambda$  to 9.5 nm. Coatings developed a dense multilayer structure. According to the GI-XRD and TEM observations, WN layers consisted of a face-centered cubic (fcc)  $\beta$ -W<sub>2</sub>N phase. The NbN layers were composed of the fcc  $\delta$ -NbN and hexagonal  $\varepsilon$ -NbN phases. It was found that lattice constants decreased with an increase in the  $U_s$ . Moreover, the calculated average crystallite sizes slightly decreased for all phases from approximately 2.3 to 5.0 nm. Coating deposited at -50 V exhibited the best mechanical properties and wear resistance: hardness of 35.2  $\pm$  3.3 GPa, elastic recovery of 55%, H/E = 0.085, H<sup>3</sup>/E<sup>2</sup> = 0.254, friction coefficient of 0.73, and specific wear rate of about 1.01  $\cdot$  10<sup>-6</sup> mm<sup>3</sup>/N·m. The combination of all these factors makes new CA-PVD WN/NbN coatings suitable candidates for protecting cuttings tools.

#### Transparent ceramics of LiAl<sub>5</sub>O<sub>8</sub> prepared by spark plasma sintering

<u>Tomáš Thoř</u><sup>1,2</sup>, Kateřina Rubešová<sup>1</sup>, Vít Jakeš<sup>1</sup>, and Filip Průša<sup>3</sup>

<sup>1</sup>Department of Inorganic Chemistry, University of Chemistry and Technology Prague, Technická 5, 166 28 Praha 6, Czech Republic

<sup>2</sup>TOPTEC Centre, Institute of Plasma Physics of the Czech Academy of Sciences, Sobotecká 1660, 51101 Turnov, Czech Republic

<sup>3</sup>Department of Metals and Corrosion Engineering, University of Chemistry and Technology Prague, Technická 5, 166 28 Praha 6, Czech Republic

Transparent ceramics are a relatively new material form that serves as an alternative to the traditionally encountered glasses, polymers or highly transparent single crystals. They have found application in a variety of optical and electro-optical devices such as solid state lasers and scintillators, but also in some non-optical applications, e.g. armours. The fabrication of transparent ceramics usually involves a combination of chemical and physical processes, which are used to prepare a ceramic powder and compact the powder into a dense ceramic body. However, the optical properties of finished polycrystalline ceramics are closely related to their microstructure and to the presence of defects in it. Residual pores (located within grains or at grain boundaries), impurities or the actual grain boundaries (especially for optically anisotropic materials) are sources of light scattering, which deteriorates the optical properties of transparent ceramics. Therefore, transparent ceramics are commonly prepared from materials with an optically isotropic cubic structure using high purity powders, which leave porosity as the most significant factor for transparency.

In this work, the preparation of  $LiAl_5O_8$  transparent ceramics is presented using spark plasma sintering (SPS). Powder precursors were prepared using two methods, namely the solgel method and the solid state reaction. Before sintering, the powders were heat treated at a high temperature of 1100 or 1200 °C and their phase composition was verified by XRD to be a pure cubic  $\alpha$ -phase of  $LiAl_5O_8$ . The powders were compacted into dense ceramic bodies by SPS, which were further processed by grinding and polishing to achieve a mirror finish and a thickness of approximately 1 mm. The transmittance and microstructure of the sintered ceramics were investigated to determine optimal conditions for the powder preparation and its sintering. Transparent ceramics with transmittance greater than 75 % at 500 nm was achieved.

### The influence of heat treatment on the nitriding layear on AISI 304 austenitic steel

<u>Milan Uhríčik</u>, Peter Palček, Viera Zatkalíková, Lenka Markovičová, Silvia Hudecová, Zuzana Šurdová, Martin Slezák, and Veronika Chvalníková

University of Žilina, Univerzitná 8215/1, Žilina 01026, Slovakia

Nitriding is a technology that leads to an increase in the utility value of the product. It's most important benefits include increased corrosion resistance, abrasion resistance, wear resistance, increased resistance to fatigue failure under cyclic loading, and many others. The design of a suitable nitriding technology not only on the basis of empirics requires a closer study of the relationship between the structure of the nitriding layer, its properties and the course of a particular degradation process. Because the life of most components is related to abrasion on the surface, the occurrence of fatigue cracks and corrosion effects, it is crucial to influence the mechanical and other properties in this surface area [1].

Plasma nitriding is the technological peak of the nitriding procedure and provides considerable advantages as compared to the salt bath and gas nitriding. Components and tools with a plasma nitrided surface show improved wear resistance, better friction and sliding properties, and higher fatigue strength values [2].

The article will be focused on the analysis of the influence of heat treatment on the nitriding layer, which will be applied on austenitic steel. AISI 304 austenitic steel delivered without heat treatment will be used as experimental material. The nitriding layer will be applied to the austenitic steel samples by plasma nitriding. Then, after plasma nitriding, samples will be subjected to heat treatment. Solution annealing and sensitization will be chosen as heat treatment.

Experiments deal with microstructural material analysis, fractographic analysis, mechanical and fatigue tests. The microstructure of the testing sample was examined using a light microscope. Fatigue properties of austenitic steel were tested by three-point bending cyclic loading. The fracture surface of the testing sample was examined using a scanning electron microscope, where samples were observed on various stages of the fatigue process, their characteristics and differences of fracture surfaces. An important indicator will also be the measurement of hardness, or the change in the course of hardness.

- [1] D. Dobrocký, Z. Joska, J. Procházka, E. Svoboda, and P. Dostál, Man. Tech. 21 (2021) 183.
- [2] E. Roliński, G. Sharp, and A. Konieczny, Heat Trea. Prog. 6 (2006) 19.

#### **Development of novel cross-luminescence scintillators**

Vojtěch Vaněček, Robert Král, Romana Kučerková, Petra Zemenová, and Martin Nikl

Institute of Physics of Czech Academy of Sciences, Cukrovarnická 10/112, Praha, Czechia

Scintillators find application in many areas of human activity including medicine, geology, national security, and environmental protection. A large number of scintillators are produced on an industrial level and commercially available, for example, classical scintillators like NaI:Tl, CsI:Tl, Bi<sub>4</sub>Ge<sub>3</sub>O<sub>12</sub>, and Y<sub>3</sub>Al<sub>5</sub>O<sub>12</sub>:Ce or state-of-the-art scintillators like (Lu, Y)<sub>2</sub>SiO<sub>5</sub>:Ce, Gd<sub>3</sub>(Ga, Al)<sub>5</sub>O<sub>12</sub>:Ce, and LaBr<sub>3</sub>:Ce,Sr. However, new technical challenges, primarily from the fields of medical imaging and high-energy physics, require timing performance that these scintillators cannot fulfill. Therefore, new so-called "ultrafast" scintillators must be developed. One of the material groups promising ultrafast scintillators are cross-luminescence scintillators. Cross-luminescence is a fast radiative recombination between electron in the valence band and hole in the uppermost core band. It was first observed as a fast component of the scintillation pulse of BaF<sub>2</sub> single crystals in 1982. Since then, it has been intensively researched, but found little industrial application, mainly due to its emission in the deep UV. Nevertheless, cross-luminescence scintillators based on cesium chloride and fluoride could overcome this problem by redshift of the emission. Moreover, complex compositions containing heavy elements could decrease attenuation length for high-energy photons which is a crucial parameter in medical imaging. In this contribution, I will present my work on the development of a novel cross-luminescence scintillator and outline perspectives/obstacles for future development.

# Er-doped zinc-silicate glass-ceramics with enhanced emission in the near-infrared region

<u>Petr Vařák</u><sup>1,2</sup>, Jan Baborák<sup>1</sup>, Emmanuel Véron<sup>3</sup>, Alena Michalcová<sup>4</sup>, Jan Mrázek<sup>2</sup>, Jakub Volf<sup>1</sup>, Mathieu Allix<sup>3</sup>, and Pavla Nekvindová<sup>1</sup>

<sup>1</sup>Department of Inorganic Chemistry, University of Chemistry and Technology, Technická 5, 166 28, Prague, Czech Republic

<sup>2</sup>Institute of Photonics and Electronics of the Czech Academy of Sciences, Chaberská 1014/57, 182 51 Prague, Czech Republic

<sup>3</sup>CNRS, CEMHTI UPR3079, Univ. Orléans, F-45071 Orléans, France

<sup>4</sup>Department of Metals and Corrosion Engineering, University of Chemistry and Technology,

Technická 5, 166 28, Praque, Czech Republic

Glass-ceramics from the system  $A_2O$ -ZnO-SiO<sub>2</sub> (A = Li, Na, K, Cs) were prepared, and the relationship between the composition, crystallization and luminescence properties is studied. The glass-ceramics contain various crystalline phases, including zinc oxide ZnO, zinc silicate Zn<sub>2</sub>SiO<sub>4</sub> (willemite) or alkali zinc silicate A<sub>2</sub>ZnSiO<sub>4</sub>. We show that the tendency towards crystallization increases with decreasing diameter of alkali cation, from Cs<sup>+</sup> to Li<sup>+</sup>. The Li<sub>2</sub>Ocontaining glass crystallizes directly after melt-quenching, whereas the Cs<sub>2</sub>O-containing glass only crystallizes after heat treatment at 900 °C. We show that the Na<sub>2</sub>O-ZnO-SiO<sub>2</sub> system is highly beneficial for the crystallization of willemite. The presence of Zn<sub>2</sub>SiO<sub>4</sub> nanocrystals in the Na<sub>2</sub>O-containing samples is confirmed by TEM imaging, the size of nanocrystals is around 8 nm. The high crystallinity of the samples leads to a significant enhancement of emission intensity around 1.5  $\mu$ m. However, the solubility of Er<sup>3+</sup> ions in the zinc-based crystalline phases is shown to be highly limited. When heat treated in the range of 700 - 850 °C, the luminescence characteristics of the 1.5  $\mu$ m emission, such as band shape or fluorescence lifetime remain nearly unchanged or exhibit only small modifications, suggesting negligible changes in the Er<sup>3+</sup> environment. The Er<sup>3+</sup> ions likely remain in the residual amorphous phase or grain boundaries. A significant evidence for the incorporation of Er<sup>3+</sup> ions in crystalline lattice is observed only in samples heat treated at 900 °C, where the Na<sub>3</sub>ErSi<sub>3</sub>O<sub>9</sub> phase is formed in the Na<sub>2</sub>O-ZnO-SiO<sub>2</sub> system.

## The effect of composition on luminescence properties of Ce and Mn ions in borate-silicate glasses

<u>Jakub Volf</u><sup>1</sup>, Petr Vařák<sup>1</sup>, Martin Kormunda<sup>2</sup>, Maksym Buryi<sup>3</sup>, and Pavla Nekvindová<sup>1</sup>

This contribution is focused on preparation of luminescent borosilicate glass able to improve intensity of UV-VIS solar radiation simultaneously in blue and red regions in order to support the growth of single-cell algae. Borate and borosilicate glasses doped with ions Ce<sup>3+</sup> and  $\mathrm{Mn}^{2+}$  were studied and a trade-off was found between luminescent properties and chemical resistance. The relationship between the oxidation states of the elements and the composition of the glass matrix was sought. Specifically, the effect of Mn concentration and content of network modificators (MgO, CaO, BaO) on strengthening of luminescence in the red region was studied in relation to optical basicity ( $\Lambda$ ), which is an essential parameter affecting redox equilibrium and consequently the luminescence of glass. The optical basicity (  $\Lambda$ ) was calculated from oxide contents in glasses and compared with experimental values obtained by use of Lorentz-Lorenz relation and Duffy correlation. Refractive indices and densities of glasses needed were obtained by means of m-line spectroscopy and pycnometry. The oxidation states of cerium and manganese were studied by XPS and EPR. Absorption and fluorescence spectra in UV- VIS region were also measured. Fluorescence spectra were measured for vast ranges of excitation and emission wavelengths then the measurement was repeated for chosen wavelengths with greater precision. The results show that the silicate glass containing 15% of B<sub>2</sub>O<sub>3</sub> and 1% of MnO possesses measurable luminescence in blue and red region under 320 nm excitation. The intensity of luminescence can be affected by change of optical basicity of glass matrix, however the luminescence in red region is still too weak for practical application.

<sup>&</sup>lt;sup>1</sup>Department of Inorganic Chemistry, University of Chemistry and Technology, Technicka 5, 166 28 Prague 6, Czech Republic

<sup>&</sup>lt;sup>2</sup>Department of Physics, Jan Evangelista Purkyně University in Ústí nad Labem Pasteurova 3544/1, 400 96 Ústí nad Labem, Czech Republic

<sup>&</sup>lt;sup>3</sup>Department of Optical Materials, Institute of Physics of the Czech Academy of Sciences, Na Slovance 1999/2182 00 Prague 8, Czech Republic

### Development of cutting forces in high-speed machining on turning centre

Tomáš Vopát, František Jurina, Marek Vozár, Boris Pätoprstý, and Martin Necpal

Slovak University of Technology in Bratislava, Faculty of Materials Science and Technology in Trnava, , Jana Bottu 25, Trnava, Slovakia

The article deals with the investigation of high-speed machining. The influence of cutting speed on the development of individual cutting forces components in turning was determined. Cutting tests were carried out on turning centre during the machining of C45 medium carbon steel material. The cutting tool material was cubic nitride boron. Cutting speed was selected with respect to the high-speed machining. In the experiment, time monitoring of cutting forces was recorded. From the results, a decreasing trend in the cutting forces values was observed from the cutting speed higher than 1100 m/min.

## Influence of cutting edge microgeometry on the selected aspects of machining difficult-to-cut materials

Marek Vozár, Boris Pätoprstý, Tomáš Vopát, Ivan Buranský, and František Jurina

Faculty of Materials Science and Technology in Trnava, Slovak University of Technology in Bratislava, Ulica Jána Bottu 25, 91724 Trnava, Slovakia

The paper presents research investigating the influence of cutting tools microgeometry on the cutting forces and machined surface roughness when milling different-to-cut materials. Austenitic stainless steel AISI 316L and nickel alloy Inconel 718 were machined with cemented carbide tools with various cutting edge rounding size while measuring the cutting forcess during the process and machined surface roughness after the machining. From the standpoint of milling difficult-to-cut materials lowering the cutting forces load on the tool as well as attaining sufficient quality of machined surface can be difficult to achieve. Previous research into the cutting edge microgeometry suggests that modification of the cutting edge of milling tools can substantially extend the effective tool life, reduce cutting forces in the process and ensure higher quality of the machined surface. Results of long term wear tests of tools with cutting edge rounding sizes of 15, 30 and 45  $\mu$ m are compared to the results of a sharp unprepared cutting tool, and the results of each machined material are also compared. Possible influence of cutting edge radius on the process for both materials was tested for cutting conditions constituting finishing operation. The most effective cutting edge radius size differed between the materials, with 15  $\mu$ m rounding performing the best for AISI 316L and the sharp unprepared tool performing the best for the Inconel 718 alloy.

# Composition Dependence of Resistivity of Ru-Mo-W ternary system and single crystal wire growth by the dewetting micro-pulling-down method

Kotaro Yonemura<sup>1,2</sup>, Rikito Murakami<sup>2</sup>, Shiika Itoi<sup>3</sup>, Kei Kamada<sup>3,4</sup>, Takahiko Horiai<sup>4</sup>, Takashi Hanada<sup>2</sup>, Akihiro Yamaji<sup>4</sup>, Masao Yoshino<sup>4</sup>, Hiroki Sato<sup>4</sup>, Yuji Ohashi<sup>4</sup>, Shunsuke Kurosawa<sup>4</sup>, Yuui Yokota<sup>2</sup>, and Akira Yoshikawa<sup>2,3,4</sup>

<sup>1</sup>Graduate School of Engineering, Tohoku University, Sendai, Japan
<sup>2</sup>Institute for Materials Research, Tohoku University, Sendai, Japan
<sup>3</sup>C&A Corporation, Sendai, Japan
<sup>4</sup>New Industry Creation Hatchery Center, Tohoku University, Sendai, Japan

Recently, we have developed Ru-Mo-W single crystal alloy wires (Ruscaloy) by the dewetting micro-pulling-down (  $\mu$ -PD) method<sup>[1]</sup> for the heaters of the vacuum evaporation method. Ruscaloy have higher electrical resistivity and approximately three times longer lifetime than that of Ta at 1873 K.  $\mu$ -PD method causes macro segregation during crystal growth, therefore the Mo and W composition of wire may be different from the target composition. However, the relationship between composition change and crystallization yield of the alloy wire has been incompletely understood. Moreover, composition change may change resistivity. In Ru-Mo and Ru-W binary system, resistivities change in accordance with the Nordheim law<sup>[2]</sup>. However, the relationship between composition change and resistivities change of Ru-Mo-W ternary system has not been studied. In this study, we investigated the composition with macro segregation of Ruscaloy and the composition with resistivities of Ru-Mo-W ternary alloys along with their compositional change to suggest acceptance criteria for maintaining Ruscaloy quality.

 $Ru_{1-x-y}Mo_xW_y$  (x = 0 to 0.42, y = 0 to 0.42) polycrystalline alloys were synthesized using an arc melting furnace with the raw materials of >99.9% purity.  $Ru_{60}Mo_{15}W_{25}$  single crystal wire was growthed by dewetting  $\mu$ -PD method. After the heat treating at 2273 K for 3 hours in high purity Ar atmosphere, wire specimens were cut from different crystallization yield and measured their composition. The resistivities of polycrystalline alloy specimens were measured by the 4-terminal method to investigate the relationship between composition and resistivity despite the effect of crystal anisotropy. A quadratic surface of the composition-resistivity relationship was fitted on the ternary diagram.

 $Ru_{60}Mo_{15}W_{25}$  alloy wire with diameters of 0.78-0.80 mm was grown by controlling the maximum pulling-down rate at 100 mm/min. The wire had smooth sides and a stable circular cross-section. The length of the grown wire was 8.04 m and maximum crystallization yield was 45.6 %. The resistivities of polycrystalline specimens increased with both Mo and W composition. Resistivity change with W composition increase was higher than Mo. The details of the wire composition with crystallization yield will be presented.

- [1] R. Murakami, A. Yoshikawa et al., ACS Omega. 6 (2021), 8131-8141.
- [2] R. Murakami, A. Yoshikawa et al., Int. J. Refract. Met. Hard Mater. 114 (2023) 106235.

## Corrosion resistance of austenitic stainless steels in mixed sulfuric acid and copper sulfate solution

Viera Zatkalíková, Lenka Markovičová, Milan Uhríčik, and Silvia Hudecová

University of Žilina, Univerzitná 8215/1, 010 26 Žilina, Slovakia

Austenitic stainless steels are widely used not only for common domestic, industrial, transport and architectural applications, but they are also acceptable as a construction material across the chemical-processing and petrochemical industries. It is due their ability to withstand attack from highly corrosive substances when they are in the passive state, as well as their effective mechanical characteristics. However, it is necessary to take into account, that stainless steels have some important limits in their corrosion resistance. In addition to the susceptibility to the local pitting corrosion in chloride containing media they may also suffer from the intergranular corrosion. This corrosion form usually takes place in aggressive environments after sensitization by thermal exposure in critical temperatures with consequent slow cooling in the air. Under these conditions,  $M_{23}C_6$  chromium-rich carbides precipitate on the grain boundaries. It causes a drop of the chromium content near the grain boundaries under the passivity limit and chromium depleted zones become the preferential paths for pitting corrosion attack.

Stainless steels generally offer good resistance to the corrosion in sulfuric acid, but the level of their resistance varies depending on the grade of the used steel and the concentration and temperature of the sulfuric acid. The presence of oxidizing or reducing contaminants, velocity effects and solids in suspension also affect the aggressiveness of this acid toward the stainless steels. At ambient temperature, austenitic stainless steels exhibit stabile passivity state in highly concentrated sulfuric acid (above 93 %) and they are frequently used for piping and tankage where product purity is desirable. In dilute sulfuric acid solutions, molybdenum containing grades exhibit higher corrosion resistance than Cr-Ni steels. However, diluted sulfuric acid solutions are considered the environments that can induce intergranular corrosion of austenitic stainless steel. The aggressiveness of these solutions in relation to the intergranular corrosion can be increased if mixed with copper sulfate due to the catalytic effect of copper ions and promoting the precipitation of copper-rich phases at the grain boundaries

This study is focused on the evaluation of AISI 304 and AISI 316L stainless steels corrosion resistance in mixed 10 wt. % sulfuric acid and 10 wt. % copper sulfate solution. Sensitized (650 °C /40 hours) and solution annealed (1050 °C /15 min) specimens together with the untreated (as received) ones are examined by long-term (22-month) exposure immersion test at the temperature of  $22 \pm 3$  °C on the bases of optical microscopy and SEM. Both tested stainless steels in as received and solution annealed state proved high corrosion resistance in the given corrosive environment. The cross-sections edges of sensitized specimens revealed a close relationship between local corrosion sites and weakened grain boundaries. The observed damage indicates incipient intergranular corrosion.

### **Author Index**

#### Α Abe Yuka, 15 Falvey Alexandra, 42 Allix Mathieu, 18, 67 G Artemenko Anna, 21 Gerhátová Žaneta, 28 Guguschev Christo, 33 Babalová Eva, 16, 20 Η Babčenko Oleg, 17, 59 Hájek František, 21 Babin Vladimir, 21 Hanada Takashi, 15, 54, 71 Babincová Paulína, 28 Haršáni Marián, 63 Baborák Jan, 18, 67 Havlíček Jan, 29, 56 Bartosiewicz Karol, 19 Horiai Takahiko, 15, 19, 30, 36, 54, 71 Behúlová Mária, 16, 20 Hostinský Tomáš, 31, 40 Beitlerová Alena, 29 Hubáček Tomáš, 21 Beňo Matúš, 25 Hudáková Mária, 28 Beranová Klára, 17 Hudecová Silvia, 32, 47, 65, 72 Beresnev Vyacheslav, 63 Ι Bočáková Barbora, 37, 43, 61 Itoi Shiika, 50, 71 Bucha Peter, 51 Budjač Roman, 46 J Buranský Ivan, 55, 70 Jakeš Vít, 29, 33, 60, 64 Buryi Maksym, 21, 34, 59, 68 Janovec Jozef, 23 Bystřický Aleš, 42 Jelínková Helena, 56 John David, 34 $\mathbf{C}$ Jozefíková Flóra, 58 Čaplovič Lubomír, 63 Jurina František, 35, 55, 69, 70 Čaplovičová Mária, 63 Casares Antonio, 22 Čermák Jan, 17 Kamada Kei, 15, 36, 50, 54, 71 Černičková Ivona, 23, 27 Kim Kyoung Jin, 54 Červeňanská Zuzana, 39 Knedlová Jana, 37, 43 Chvalníková Veronika, 32, 65 Kolařík Ladislav, 61 Čička Roman, 24, 27 Kolaříková Marie, 61 Kolářová Kateřina, 17 $\mathbf{D}$ Koman Marian, 38 Dobrovodský Jozef, 25 Kormunda Martin, 68 Dobrovodský Ladislav, 27 Kotianová Janette, 39 Drienovský Marián, 27 Koudelka Ladislav, 31, 40 Ďuriš Rastislav, 26, 39 Kovačócy Pavel, 49 Ďuriška Libor, 23, 27

Kožíšek Zdeněk, 41

Krajčovič Jozef, 24 P Pachnerová Brabcová Kateřina, 34 Král Robert, 41, 42, 66 Palček Peter, 32, 65 Kromka Alexander, 17 Kubišová Milena, 37, 43 Palcut Marián, 28 Kučerková Romana, 29, 33, 66 Pata Vladimír, 37, 43 Paták Jozef, 28 Kuchtanin Vladimír, 44 Pätoprstý Boris, 35, 55, 69, 70 Kurosawa Shunsuke, 15, 19, 54, 71 Kusy Martin, 63 Pavlik Ján, 44 Pejchal Jan, 33, 42, 56, 59 Kutsuzawa Naoko, 36 Piasecki Michal, 57  $\mathbf{L}$ Pitcher Michael, 18 Labašová Eva, 26 Pogrebnjak Alexander, 63 Laguta Oleksii, 45 Prikner Jiří, 33 Lofaj František, 25 Prošek Zdeněk, 17 Průša Filip, 64 M Puchoňová Miroslava, 58 Marcaník Miroslav, 37 Markechová Iveta, 46 R Marko Andriy, 45 Remeš Štěpán, 59 Markovičová Lenka, 32, 47, 65, 72 Remeš Zdeněk, 17, 21, 59 Maroszová Jaroslava, 48 Riedlmajer Robert, 25 Martinkovič Maroš, 49 Rolník Ladislav, 51 Michalcová Alena, 67 Rubešová Kateřina, 29, 33, 60, 64 Mičová Júlia, 21, 59 S Mikolajčík Martin, 32 Sahul Martin, 61, 63 Moncol' Ján, 44 Sahul Miroslav, 61 Moravčík Roman, 27 Santana Vinicius, 45 Mošner Petr, 31, 40 Sasaki Rei, 36 Mrázek Jan. 67 Sato Hiroki, 15, 54, 71 Murakami Rikito, 15, 50, 54, 71 Šedivý Matuš, 45 N Shirakami Yuji, 36 Nad' Milan, 51 Šimna Vladimír, 62 Necpal Martin, 52, 69 Slezák Martin, 32, 65 Nejezchleb Karel, 56 Smyrnova Kateryna, 63 Nekvindová Pavla, 18, 67, 68 Stúpalová Hana, 46 Němec Tomáš, 61 Šulc Jan, 56 Nesladek Milos, 53 Šurdová Zuzana, 65 Neugebauer Petr, 45 Švec sr. Peter, 23 Nikl Martin, 29, 33, 42, 56, 66 Světlík Ivo, 34 Novák Radim, 59 Szymanski Damian, 19 O

Tesárek Pavel, 17

Thoř Tomáš, 33, 64

#### 74

Ohashi Yuji, 15, 54, 71

Omuro Kazuya, 54

### Turza Michal, 39

#### U

Uhríčik Milan, 32, 47, 65, 72 Usuki Yoshiyuki, 36

#### $\mathbf{V}$

Vaňa Dušan, 25 Vaněček Vojtěch, 42, 66 Vařák Petr, 18, 67, 68 Varga Rudolf, 44 Veron Emmanuel, 18 Véron Emmanuel, 67 Volf Jakub, 67, 68 Vopát Tomáš, 35, 55, 69, 70 Vozár Marek, 35, 55, 69, 70 Vrbová Hana, 43

#### W

Witkowski Marcin, 19

### Y

Yamaji Akihiro, 15, 54, 71 Yokota Yuui, 15, 30, 54, 71 Yonemura Kotaro, 50, 71 Yoshikawa Akira, 15, 19, 30, 36, 50, 54, 71 Yoshino Masao, 15, 19, 30, 36, 54, 71

#### Z

Zandona Alessio, 18 Zatkalíková Viera, 32, 47, 65, 72 Zemenová Petra, 41, 42, 66

### LIST OF PARTICIPANTS

Miss. Yuka Abe

Institute for Materials Research, Tohoku University

2-1-1 Katahira, Aoba-ku

Sendai, Miyagi

Japan

Dr. Mária Behúlová

Slovak University of Technology in Bratislava

Faculty of Materials Science and Technology in Trnava

Ulica Jána Bottu č. 2781/25

917 24 Trnava

Slovakia

Dr. Eva Babalová

Slovak University of Technology in Bratislava

Faculty of Materials Science and Technology in Trnava

ul. Jána Bottu Č. 2781/25

Trnava 91724 Slovakia Dr. Barbora Bočáková

Slovak University of Technology

Faculty of materials science and technology

J. Bottu 24

Trnava

Slovakia

Dr. Oleg Babčenko

FZU - Institute of Physics of the Czech Academy of Sci-

ences

Cukrovarnická 10/112 162 00 Prague 6

Czechia

Mr. Jakub Brož

University of Chemistry and Technology

Technická 5 Praha 6

Czechia

Mr. Jan Baborák

University of Chemistry and Technology

Department of Inorganic Chemistry

Technická 5

Prague 6 Czechia Dr. Maksym Buryi

FZU - Institute of Physics of the Czech Academy of Sci-

ences

Cukrovarnická 10/112

Prague

Czechia

Dr. Karol Bartosiewicz

Faculty of Physics of Kazimierz Wielki University

Powstańców Wielkopolskich 2

85-090 Bydgoszcz

Poland

Dr. Antonio Casares Carl Zeiss spol. s r.o.

Radlická 14/3201

Praha Czechia Dr. Ivona Černíčková

Faculty of Materials Science and Technology in Trnava

Slovak University of Technology in Bratislava

Jána Bottu 2781/25 Trnava 91724 Slovakia Dr. Žaneta Gerhátová

Faculty of Materials Science and Technology in Trnava,

Slovak University of Tech

Jána Bottu 25 Trnava

Slovakia

Dr. Roman Čička

Faculty of Materials Science and Technology, Slovak

University of Technology

J. Bottu 25

Trnava, 917 24

Slovakia

Mr. Jan Havlíček

VŠCHT Praha, Ústav anorganické chemie

Technická 5

166 28 Praha 6

Czechia

Dr. Jozef Dobrovodský

Slovak University of Technology in Bratislava

Faculty of Materials Science and Technology in Trnava

Jána Bottu č. 2781/25

917 24 Trnava

Slovakia

Dr. Takahiko Horiai

Institute for Materials Research, Tohoku University

2-1-1 Katahira, Aoba-ku

Sendai, Miyagi

Japan

Dr. Rastislav Ďuriš

Slovak University of Technology

Faculty of Materials Science and Technology

jána Bottu 25

Trnava, 917 24

Slovakia

Mr. Tomáš Hostinský

University of Pardubice, Faculty of Chemical Technol-

ogy

Department of General and Inorganic Chemistry

Studentská 573

Pardubice 532 10

Czechia

Dr. Libor Ďuriška

Faculty of Materials Science and Technology in Trnava

Slovak University of Technology in Bratislava

Jána Bottu 2781/25

Trnava 91724

Slovakia

Dr. Silvia Hudecová University of Žilina

Department of Materials Engineering

Univerzitná 8125/1

Žilina

Slovakia

Dr. Vít Jakeš

University of Chemistry and Technology

Technická 5

Praha 6 Czechia Dr. Jana Knedlová

Tomas Bata University in Zlín

Vavrečkova 5669

Zlín Czechia

Mr. David John

Institute of Physics of the Czech Academy of Sciences

Cukrovarnická 10/112 Praha 6, 162 00 Czechia Prof. Marian Koman Slovak Technical University

Faculty of Chemical and Food Technology STU in

Bratislava Radlinského 9 Bratislava Slovakia

Dr. František Jurina

MTF STU

Ulica Jána Bottu č. 2781/25 Trnava Slovakia Dr. Janette Kotianová

Slovak University of Technology in Bratislava

Bottova 25 Trnava Slovakia

Prof. Kei Kamada

Institute for Materials Research, Tohoku University

2-1-1 Katahira

Sendai

Japan

Prof. Ladislav Koudelka University of Pardubice

Studentska 95

University of Pardubice

Pardubice Czechia

Dr. Miroslav Kamensky

TESTOVACI TECHNIKA s.r.o.

Československé armády 923

Poděbrady Czechia Dr. Zdeněk Kožíšek

Institute of Physics of the Czech Academy of Sciences

Cukrovarnická 10 162 00 Praha 6 Czechia Dr. Robert Kral

Institute of Physics, Czech Academy of Sciences

Cukrovarnicka 10

Prague Czechia Dr. Iveta Markechová

Slovak Uni Technol, Fac Mater Sci & Technol, Dept

Appl Math

Jána Bottu 2781/25 917 24 Trnava Slovakia

Dr. Kristýna Králová Faculty of Arts Charles University nám. J. Palacha 1/2

Prague 1 Czechia Dr. Lenka Markovičová University of Žilina Univerzitná 8215/1

Žilina Slovakia

Dr. Milena Kubišová

Tomas Bata University in Zlín, Faculty of Technology

Vavrečkova 5669

Zlín Czechia Dr. Jaroslava Maroszová

Faculty of Chemical and Food technology, STU in

Bratislava, Slovakia Radlinského 9 Bratislava Slovakia

Dr. Vladimír Kuchtanin

Slovak University of Technology in Bratislava,

Bratislava, Slovak Republic

Radlinského 9 Bratislava Slovakia Prof. Maroš Martinkovič

Faculty of Material Science and Technology SUT, Tr-

nava, Slovak Republic

J. Bottu 25 Trnava Slovakia

Dr. Oleksii Laguta

VUT Brno

Purkynova 123 Brno, 61200

Czechia

Dr. Rikito Murakami

Institute for Materials Research, Tohoku University

2-1-1, Katahira Sendai, Miyagi

Japan

Mr. Milan Nad'

Slovak University of Technology

Faculty of Materials Science and Technology

Ul. J. Bottu 25 917 24 Trnava Slovakia Dr. Jan Pejchal

Institute of Physics, Czech Academy of Sciences

Cukrovarnicka 10

Prague Czechia

Dr. Martin Necpal

MTF STU

Ul. Jána Bottu

Trnava Slovakia Prof. Michal Piasecki

Jan Dlugosz University in Czestochowa

Armii Krajowej 13/15

Czestochowa Poland

Prof. Milos Nesladek Hasselt University

Martelarenlaan 42

Hasselt Belgium Dr. Miroslava Puchoňová

Faculty of Chemical and Food technology, STU in

Bratislava Radlinského 9 Bratislava Slovakia

Mr. Kazuya Omuro Tohoku Univ.

Institute for Materials Research, Tohoku University

2-1-1 Katahira, Aoba-ku,

Sendai, Miyagi Japan Dr. Zdeněk Remeš

FZU - Institute of Physics of the Czech Academy of Sci-

ences

Na Slovance 1999/2

Prague 8 Czechia

Dr. Boris Pätoprstý

Faculty of Materials Science and Technology in Trnava Slovak University of Technology in Bratislava

Ulica Jána Bottu č. 2781/25

Trnava 917 24 Slovakia Dr. Kateřina Rubešová

University of Chemistry and Technology

Technická 5 Praha 6 Czechia Dr. Martin Sahul

Faculty of Materials Science and Technology, Slovak

University of Technology

Bottova 25 Trnava Slovakia Dr. Milan Uhríčik University of Žilina Univerzitná 8215/1 Žilina 01026

Dr. Vladimír Šimna

STU MTF Trnava

Ústav Výrobných Technológií

Bottova 25 917 24 Trnava Slovakia Mr. Vojtěch Vaněček

Institute of Physics of Czech Academy of Sciences

Cukrovarnická 10/112

Praha Czechia

Slovakia

Dr. Kateryna Smyrnova

Faculty of Materials Science and Technology, Slovak

University of Technology in Bratislava Jána Bottu, 25

917 24 Trnava Slovakia Dr. Petr Vařák

University of Chemistry and Technology

Technická 5 Praha 160 00 Czechia

Mr. Tomáš Thoř University of Chemistry and Technology

Technická 5 Prague 6 Czechia Mr. Jakub Volf UCT Prague Technická 5 Praha, 160 00 Czechia

Mr. Vít Tichý

**ZEISS Research Microscopy Solutions** 

Carl Zeiss spol. s r.o. Radlická 14/3201 150 00 Praha 5 Czechia Dr. Tomáš Vopát

Faculty of Materials Science and Technology, Slovak

University of Technology

Jana Bottu 25 Trnava Slovakia Dr. Marek Vozár Faculty of Materials Science and Technology in Trnava Slovak University of Technology in Bratislava Ulica Jána Bottu 25 91724 Trnava Slovakia

Mr. Kotaro Yonemura Institute for Materials Research, Tohoku University 2-1-1 Katahira, Aoba-ku Sendai, Miyagi Japan

Dr. Viera Zatkalíková University of Žilina Univerzitná 8215/1 010 26 Žilina Slovakia